

DESIGN AND ANALYZE OF LIGHTNING DETECTION FOR A LOW-COST SYSTEM

MUHAMMAD ZULFARHAN BIN MOHD SABRI



UNIVERSITI TEKNIKAL MALAYSIA MELAKA

**DESIGN AND ANALYZE OF LIGHTNING DETECTION
FOR A LOW-COST SYSTEM**

MUHAMMAD ZULFARHAN BIN MOHD SABRI

**This report is submitted in partial fulfilment of the requirements
for the degree of Bachelor of Electronic Engineering with Honours**



**Faculty of Electronics and Computer Technology and
Engineering
Universiti Teknikal Malaysia Melaka**

2024

**BORANG PENGESAHAN STATUS LAPORAN
PROJEK SARJANA MUDA II**

Tajuk Projek : Design and Analyze of Lightning Detection for A
Low-Cost System
Sesi Pengajian : 2023/2024

Saya MUHAMMAD ZULFARHAN BIN MOHD SABRI mengaku membenarkan laporan Projek Sarjana Muda ini disimpan di Perpustakaan dengan syarat-syarat kegunaan seperti berikut:

1. Laporan adalah hakmilik Universiti Teknikal Malaysia Melaka.
2. Perpustakaan dibenarkan membuat salinan untuk tujuan pengajian sahaja.
3. Perpustakaan dibenarkan membuat salinan laporan ini sebagai bahan pertukaran antara institusi pengajian tinggi.
4. Sila tandakan (✓):

SULIT*

(Mengandungi maklumat yang berdarjah keselamatan atau kepentingan Malaysia seperti yang termaktub di dalam AKTA RAHSIA RASMI 1972)

TERHAD*

(Mengandungi maklumat terhad yang telah ditentukan oleh organisasi/badan di mana penyelidikan dijalankan.)

TIDAK TERHAD

Disahkan oleh:



(TANDATANGAN PENULIS)



(COP DAN TANDATANGAN PENYELIA)

Alamat Tetap: 5-10-2, Lorong
Kelicap, Mutiara
Perdana 2, 11900
Bayan Lepas,
Pulau Pinang

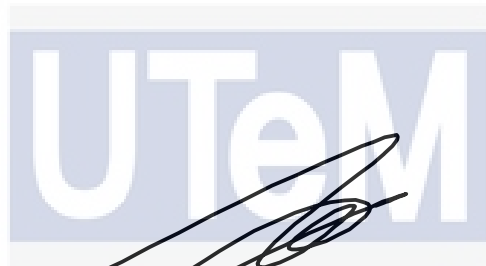
Tarikh : 24 Januari 2024

DR. NORBAYAH BINTI YUSOP
Penyarah Kanan
Fakulti Teknologi Dan Kejuruteraan Elektronik Dan Komputer (FTKEK)
Universiti Teknikal Malaysia Melaka (UTeM)

Tarikh : 25 Januari 2024

DECLARATION

I declare that this report entitled “Design and analyze of lightning detection for a low-cost system” is the result of my own work except for quotes as cited in the references.



Signature : 

Author : Muhammad Zulfarhan Bin Mohd Sabri

Date : 24 January 2024

APPROVAL

I hereby declare that I have read this thesis and in my opinion this thesis is sufficient in terms of scope and quality for the award of Bachelor of Electronic Engineering with Honours.



اونيور سبتي بون كنكل مليسيا ملاك

Signature : 

UNIVERSITI TEKNIKAL MALAYSIA MELAKA

Supervisor Name : Dr Norbayah Binti Yusop

Date : 24 January 2024

DEDICATION

I dedicate this final year project report to all those who have supported and inspired me throughout this incredible journey. To my family, whose unwavering love and encouragement have been the foundation of my strength. Your belief in me has pushed me to strive for excellence and reach for the stars. This accomplishment would not have been possible without your constant support and understanding. To my supervisor and master student's member, who have shared their wisdom and expertise, guiding me through the complexities of this project. Your patience, guidance, and valuable insights have broadened my horizons and shaped me into a better professional. To the participants and individuals who generously contributed their time and insights, enabling the research and analysis for this project. Your willingness to share your knowledge and experiences has enriched this work and made it more impactful. Lastly, I dedicate this report to myself, for persevering through the long hours, challenges, and self-doubt. This project has tested my limits, taught me resilience, and honed my skills. Thank you for being a part of my journey, and may our paths continue to intersect in the pursuit of knowledge and success.

ABSTRACT

Lightning is a phenomenon that produces extraordinary power and has the potential to destroy and pose a major threat to public safety. The problem is to devise a lightning detection system capable of identifying lightning flashes. Existing lightning detection systems are typically expensive. Thus, the objective of this project is to design a low-cost lightning detection system to accurately capture lightning flashes, analyze the type of lightning flashes captured, and evaluate the performance of the system. This system was designed by developing a Fast Field buffer circuit using BUF634. Lightning detection system was fully setup by implementing Fast Field buffer circuit with parallel plated antenna to accurately detect lightning flashes. Lightning flashes data was collected within a period of one month to evaluate the characteristic and performance of the system. The system able to detect 60 negative cloud-to-ground and 51 intra-cloud lightning flashes on July 11, 2023, from 01:32:00 until 08:30:00. BUF634 and OPA633 archived 83% similarity in lightning flash detection capability. BUF634 was a 2.3 times lower peak amplitude, a 2.1 times shorter pulse duration, and 1.9 times shorter zero crossing time compared to OPA633. In conclusion, BUF634 proves capable of detecting similar types of lightning flashes, showcasing potential cost-effectiveness without compromising crucial detection capabilities.

ABSTRAK

Kilat merupakan fenomena yang menghasilkan kuasa luar biasa dan berpotensi untuk memusnahkan serta menimbulkan ancaman besar kepada keselamatan awam. Masalahnya ialah untuk mencipta sistem pengesan kilat yang mampu mengesan kilat. Sistem pengesanan kilat sedia ada biasanya mahal. Oleh itu, objektif projek ini adalah untuk mereka bentuk sistem pengesanan kilat kos rendah untuk mengesan kilat dengan tepat, menganalisis dan menilai prestasi sistem. Sistem ini direka bentuk dengan membangunkan litar penimbal medan pantas menggunakan BUF634. Sistem pengesanan kilat disediakan sepenuhnya dengan melaksanakan litar penimbal medan pantas dengan antenna bersalut selari untuk mengesan kilat kilat dengan tepat. Data kilat dikumpul dalam tempoh sebulan untuk menilai ciri dan prestasi sistem. Sistem ini dapat mengesan 60 kilat awan-ke-tanah negatif dan 51 kilat intra-awan pada 11 Julai 2023, dari 01:32:00 hingga 08:30:00. BUF634 dan OPA633 mengarkibkan 83% persamaan dalam keupayaan pengesanan kilat kilat. BUF634 menunjukkan amplitud puncak 2.3 kali lebih rendah, tempoh nadi 2.1 kali lebih pendek, dan masa lintasan sifar 1.9 kali lebih pendek berbanding dengan OPA633. Kesimpulannya, BUF634 mampu mengesan jenis kilat kilat yang serupa, mempamerkan potensi keberkesanan kos tanpa menjejaskan keupayaan pengesanan penting.

ACKNOWLEDGEMENTS

I am profoundly grateful to Almighty Allah for granting me the strength and wisdom to successfully complete my Bachelor Degree Project 1 (BENU 4972) in the Faculty of Technology and Electronics and Computer Engineering. The completion of such a significant endeavor is not possible without the support and assistance of numerous individuals. I extend my deepest appreciation to my project supervisor, Dr. Norbayah binti Yusop, whose encouragement, and expertise played a pivotal role in the successful realization of this project. I would like to express gratitude to the lecturers and master's students who generously offered their support and assistance throughout the preparation of the thesis report. Their cooperation and encouragement significantly contributed to the overall success of the project. Moreover, I am thankful to the faculty for their financial support, which enabled the procurement of necessary components and tools. Lastly, I want to acknowledge the support of my family, dear father, mother, and friends, whose moral support and encouragement were indispensable. Their unwavering belief in my abilities kept me on track, and their contributions played a significant role in the successful completion of my Bachelor Degree Project 1. To all those who have been a part of this journey, I express my sincere appreciation for your invaluable assistance and encouragement throughout this endeavor.

TABLE OF CONTENTS

Declaration	i
Approval	i
Dedication	i
Abstract	i
Abstrak	ii
Acknowledgements	iii
Table of Contents	iv
List of Figures	viii
List of Tables	xi
List of Symbols and Abbreviations	xii
List of Appendices	xiii
CHAPTER 1 INTRODUCTION	1
1.1 BACKGROUND OF PROJECT	1

1.2	PROBLEM STATEMENT	4
1.3	OBJECTIVE	5
1.4	SCOPE OF WORK	5
1.5	SIGNIFICANT OF THE PROJECT	7
1.6	THESIS ORGANIZATION	7
CHAPTER 2 BACKGROUND STUDY		9
2.1	INTRODUCTION	9
2.2	REVIEW ON LIGHTNING FLASHES	10
2.3	CHARACTERISTIC OF ANTENNA	13
2.4	REVIEW ON SPECIFICATION OF BUFFER AMPLIFIER CIRCUIT WITH THE RESULT OBTAINED.	18
2.4.1	LH0033 High-Speed Buffer Amplifier	18
2.4.2	OPA633 High-Speed Buffer Amplifier	22
2.4.3	BUF602 High-Speed Buffer Amplifier	24
2.4.4	BUF634 High-Speed Buffer Amplifier	25
2.5	PARAMETER OF CLOUD-TO-GROUND LIGHTNING FLASHES	27
2.6	SUMMARY	29
CHAPTER 3 METHODOLOGY		30
3.1	INTRODUCTION	30
3.2	METHOD OF RESEARCH	31
3.3	HARDWARE DEVELOPMENT	33

3.3.1	Designing buffer circuit.	33
3.3.2	Fabricate buffer circuit.	36
3.3.3	Calibrate buffer circuit.	38
3.4	SET UP OF LIGHTNING DETECTION SYSTEM	40
3.4.1	Designing lightning detection system.	40
3.4.2	Calibrate lightning detection system using small-scale sparks.	41
3.4.3	Lightning Measurement Setup in UTEM	43
3.5	LIGHTNING DATA COLLECTION	44
3.5.1	Identification types of lightning.	44
3.5.2	Data collection of lightning flashes	46
3.6	SUMMARY	49
CHAPTER 4 RESULTS AND DISCUSSION		50
4.1	INTRODUCTION	50
4.2	CHARACTERISTIC OF CLOUD-TO-GROUND LIGHTNING FLASHES	51
4.2.1	Negative cloud-to-ground flashes	51
4.2.2	Comparison negative cloud-to-ground lightning flashes between Fast Field 1 and Fast Field 2	52
4.2.3	Performance similarity between Fast Field 1 and Fast Field 2	54
4.2.4	The characteristic performance of return stroke between Fast Field 1 and Fast Field 2	55
4.2.5	Ratio of lightning flashes between Fast Field 1 and Fast Field 2	63

4.3	DISCUSSION	65
4.4	SUMMARY	68
CHAPTER 5 CONCLUSION AND FUTURE WORKS		69
5.1	CONCLUSION	69
5.2	FUTURE WORK	70
5.2.1	Internet of Things (IoT)	70
5.2.2	Artificial Intelligence (AI)	71
REFERENCES		73
APPENDICES		78



اونيورسيتي تيكنيكل مليسيا ملاك

UNIVERSITI TEKNIKAL MALAYSIA MELAKA

LIST OF FIGURES

Figure 2.1: Type of cloud-to-ground lightning [12]	11
Figure 2.2: Conceptual cloud charge configurations and scenarios leading to production of downward positive lightning [15].	12
Figure 2.3: Different types of lightning discharge [18]	13
Figure 2.4: Parallel flat plate antenna [19]	14
Figure 2.5: Small-scale parallel plate antenna [20]	15
Figure 2.6: Vertical whip antenna [21]	16
Figure 2.7: Electric element attached the antenna [21]	17
Figure 2.8: Electric element circuit of the system [21]	17
Figure 2.9: Schematic diagram of buffer amplifier circuit [20]	18
Figure 2.10: Measured negative lightning return stroke [20]	19
Figure 2.11: Connection of parallel plate antenna and buffer circuit [22]	20
Figure 2.12: Example of stoke flash recorded [22]	20
Figure 2.13: Example of return stoke with double peaks [22]	21
Figure 2.14: A flash consist of preliminary breakdown pulse [22]	21
Figure 2.15: Example of positive return stoke [22]	22

Figure 2.16: Circuit diagram of the buffer amplifier circuit [23]	23
Figure 2.17: Block diagram of the electric field measuring system [23]	23
Figure 2.18: Buffer amplifier circuit [25]	24
Figure 2.19: Negative cloud-to-ground lightning flash [25]	25
Figure 2.20: Measurement system of an electric field [26]	25
Figure 2.21: Electronic circuit connected to the antenna [21]	26
Figure 2.22: Example of cloud-to-ground lightning flashes [28]	27
Figure 2.23: The characteristics of a return stroke for (a) a positive cloud-to-ground and (b) a negative cloud-to-ground flash [31]	28
Figure 3.1: Flow chart of designing the low-cost lightning detection system.	32
Figure 3.2: Resistor-capacitor circuit	33
Figure 3.3: Circuit design of Fast Field buffer circuit	35
Figure 3.4: Comparison input frequency and output frequency for buffer circuit	35
Figure 3.5: Printed circuit board layout for buffer circuit	36
Figure 3.6: Fabrication process to remove unwanted copper.	37
Figure 3.7: Completed fabrication process.	37
Figure 3.8: Placing the component on printed circuit board.	38
Figure 3.9: Calibration process to evaluate the functionality of buffer circuit.	39
Figure 3.10: Signal calibration at 1MHz frequency	40
Figure 3.11: Parallel plate antenna	41
Figure 3.12: Completed system arrangement	41
Figure 3.13: Calibration using small-scale of spark.	42
Figure 3.14: Small-scale lightning flashes	42
Figure 3.15: Installation setup for Fast Field buffer circuit and antenna	43

Figure 3.16: The parameter of negative cloud-to-ground lightning flash.	45
Figure 3.17: The parameter of multiple return stroke negative cloud-to-ground lightning flash.	45
Figure 3.18: Monitoring lightning signal on 11 July 2023	47
Figure 3.19: Example of recorded lightning data on 11 July 2023 for (a) existing system (OPA633) and (b) current system (BUF634)	47
Figure 3.20: Number of recorder lightning flashes for negative cloud-to-ground and intra-cloud flashes	48
Figure 3.21: Distribution of the number of strokes per flash for negative cloud-to-ground flashes	49
Figure 4.1: The characteristic of a return stroke for (a) negative cloud-to-ground flashes with single stroke, (b) negative cloud-to-ground flashes with two return strokes, and (c) negative cloud-to-ground with three return strokes.	51
Figure 4.2: Negative cloud-to-ground flashes with single return stroke for Fast Field 1 and Fast Field 2	52
Figure 4.3: Negative cloud-to-ground flashes with two return strokes for Fast Field 1 and Fast Field 2	53
Figure 4.4: Negative cloud-to-ground flashes with three return strokes for Fast Field 1 and Fast Field 2	53
Figure 4.5: The similarity of lightning flashes between Fast Field 1 and Fast Field 2	54
Figure 4.6: Peak amplitude of single return stroke for Fast Field 1 and Fast Field 2	56
Figure 4.7: Time interval of single return stroke for Fast Field 1 and Fast Field 2	57
Figure 4.8: Peak amplitude of multiple return stroke for Fast Field 1 and Fast Field 2	58
Figure 4.9: Time interval of multiple return stroke for Fast Field 1 and Fast Field 2	59
Figure 4.10: Ratio of lightning flashes between Fast Field 1 and Fast Field 2	64

LIST OF TABLES

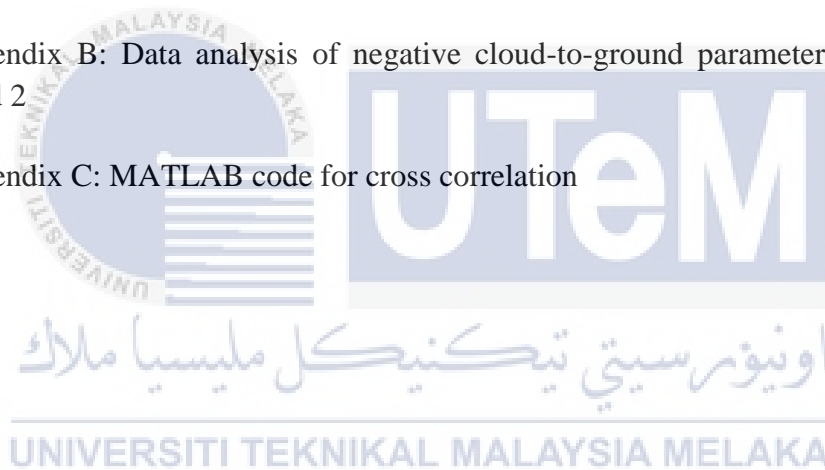
Table 4.1: Parameter of similarity between Fast Field 1 and Fast Field 2	55
Table 4.2: Peak amplitude	60
Table 4.3: Pulse duration	61
Table 4.4: Zero crossing time	61
Table 4.5: Zero-to-peak rise time	61
Table 4.6: Slow front	62
Table 4.7: Fast transition	62
Table 4.8: Inter-stroke	62
Table 4.9: Value of ratio for each parameter return stroke	64

LIST OF SYMBOLS AND ABBREVIATIONS

CC	:	Cloud-to-Cloud
IC	:	Intra-Cloud
CG	:	Cloud-to-Ground
GC	:	Ground-to-Cloud
PB	:	Preliminary Breakdown
PCB	:	Printed Circuit Board
IC	:	Integrated Circuit
FF1	:	Fast Field 1
FF2	:	Fast Field 2
-CG	:	Negative Cloud-to-Ground
+CG	:	Positive Cloud-to-Ground
FA	:	Field Antenna
IoT	:	Internet of Things
AI	:	Artificial Intelligence
RC	:	Resistor-Capacitor
E-Field	:	Electric Field

LIST OF APPENDICES

Appendix A: Data analysis of negative cloud-to-ground parameter in Fast Field 1	78
Appendix B: Data analysis of negative cloud-to-ground parameter in Fast Field 2	81
Appendix C: MATLAB code for cross correlation	83



CHAPTER 1

INTRODUCTION



1.1 BACKGROUND OF PROJECT

Lightning is a phenomenon that produces extraordinary power [1]. Lightning also has the potential to destroy and pose a major threat to public safety. With its ability to cause severe damage to electrical power devices [2], injury to people [3] and lead to casualties, and even destroy homes. Additionally, the destructive potential of lightning extends to residential and commercial properties, leading to fires and structural damage that can be financially for those affected. The development of an accurate and affordable lightning detection system is very important in protecting lives and reducing the risks associated with this natural phenomenon.

The existing lightning detection systems are typically expensive because they use advanced technology to accurately detect and locate lightning [4] [5]. Thus, this

project aims to address this critical issue by proposing a low-cost system capable of capturing lightning and analyzing the type of lightning flash. The ability to accurately detect and locate lightning strikes enables proactive measures to be taken, thereby minimizing the risks to public safety and infrastructure.

Lightning can be defined as the occurrence of a high voltage between the Earth and the clouds, resulting in the acceleration of stray electrons in the air. These accelerated electrons acquire sufficient kinetic energy to dislodge electrons from atoms in the surrounding air, causing a transient and high-current electric discharge. The path length of lightning discharges is typically measured in kilometers. Another definition of lightning is an electrical discharge taking the form of a spark within a cloud that is charged [6].

A typical lightning strike is composed of three to four strokes, although it can involve more. Each re-strike is separated by a relatively long-time interval, usually around 40 to 50 milliseconds [7]. This re-striking phenomenon creates a noticeable "strobe light" effect. Each successive stroke is preceded by intermediate dart leader strokes, which are weaker than the initial stepped leader. Typically, the succeeding strokes reuse the discharge channel established by the previous stroke. The depletion of smaller charge regions within the cloud due to successive strokes contributes to the variation in successive discharges. The sound of thunder is generated by the cumulative effect of these successive strokes in a lightning strike.

Lightning can be classified into various types based on the classifications proposed by different scientists. However, at its core, there are three primary types of lightning which are cloud-to-cloud (CC), intra-cloud (IC), cloud-to-ground (CG). When focusing on the CG, further classification can be based on polarity, resulting in

downward negative lightning, upward negative lightning, downward positive lightning, and upward positive lightning [8] [9]. CC lightning refers to lightning discharges that occur between different clouds, where each cloud carries opposite charges without directly contacting the ground. IC lightning, on the other hand, takes place within the same cloud or inside the cloud and involves interactions between areas of opposite charge. CG lightning involves a discharge between a cloud and the ground, where ions from the cloud are discharged and strike the ground. This type of lightning can involve a positive charge from the cloud hitting a negative charge on the ground. In the case of ground-to-cloud lightning, the discharge occurs between the ground and the cloud, with ions originating from the ground and striking the cloud, resulting in an interaction between charges of differing polarities [10].

In addition to the commonly known types of lightning, there exist several rare types that occur under specific conditions. One such type is beading lightning, which falls under the category of CG lightning. It is characterized by appearing to break up into bright sections and forming a string of short discharges that last longer than the typical lightning channel. Ribbon lightning is another rare type that occurs in thunderstorms with high crosswinds and multiple return strokes. The presence of strong winds causes each subsequent return stroke to be slightly displaced from the previous one, resulting in a ribbon-like appearance. Ball lightning is a fascinating phenomenon described as a floating, illuminated ball that manifests during thunderstorms [11]. It can exhibit various movement patterns, including fast, slow, or nearly stationary motion. Rocket lightning is a distinct form of cloud discharge, typically observed horizontally at the cloud base. It is characterized by a luminous channel that appears to advance through the air with perceivable speed, often intermittently.

1.2 PROBLEM STATEMENT

Lightning detection plays an important role in industries such as aviation, outdoor security, and weather monitoring. In aviation, lightning makes a serious threat to aircraft safety, and detection systems. Accurate tracking is essential for pilots to navigate safely through stormy weather conditions. Outdoor security systems rely on lightning detection to assess the risk of electrical surges and protect sensitive electronic and electrical equipment. Weather monitoring systems require lightning data to issue timely warnings and forecasts, ensuring public safety during thunderstorms.

The cost of existing lightning detection systems is quite expensive. The existing system uses high-cost components, and specialized sensors that can detect electromagnetic pulses associated with lightning [4][5]. Although these advanced systems provide accurate tracking and location capabilities, but high costs. This creates a demand for the development of alternative solutions that offer comparable accuracy and reliability at a more affordable price point. By addressing cost issues and proposing low-cost lightning detection systems, lightning detection becomes more accessible to a wider variety of users and industries. Such a system would use cost-effective components and technology and ensure accurate lightning detection.

To overcome the high cost of existing lightning detection systems and monitor lightning events, the development of low-cost alternatives can provide a solution. A low-cost lightning detection system can be designed by leveraging cost-effective components and technology without compromising accuracy and reliability. By utilizing affordable components such a system can detect and track lightning events effectively. For instance, instead of relying solely on specialized sensors, the system

can make use of existing infrastructure, such as antenna to capture electromagnetic pulses associated with lightning. By addressing the cost barriers, a low-cost lightning detection system can make lightning monitoring more accessible to a broader range of industries, ensuring the safety and security of aviation, outdoor environments, and public welfare during thunderstorms.

1.3 OBJECTIVE

The main objectives of this project are as follows:

- i. To design a low-cost lightning detection system
- ii. To analyze the types of lightning flashes.
- iii. To evaluate the characteristics of return stroke parameters.

1.4 SCOPE OF WORK

The proposed scope of work for the lightning detection system encompasses crucial elements, primarily focusing on the software utilized for designing the Fast Field buffer circuit, analyzing the types of lightning flashes, and evaluating performance of return stroke parameter. The methodology involves employing specific software tools tailored for circuit design, analysis, and evaluation of performance assessment. Furthermore, the scope includes determining the quantity of raw data used in the performance evaluation, emphasizing a data-driven approach. Another essential aspect involves evaluating the periodicity of time required to determine the system's performance, ensuring a comprehensive understanding of its effectiveness over different intervals. This holistic approach aims to leverage advanced software

applications to enhance both the design and analytical facets of the lightning detection system, providing a robust and insightful evaluation of its performance.

In the pursuit of developing a lightning detection system with the goal of capturing signals within the frequency range of 1Hz to 10MHz, a key focus lies in the design of an effective FF buffer circuit. This crucial circuit is intended to rapidly store, and process incoming electromagnetic signals associated with lightning events. The FF buffer circuit is engineered to facilitate high-speed data capture, ensuring the system's ability to accurately represent the dynamic changes in the electromagnetic field during lightning occurrences. Proteus software was used to design and simulate the FF buffer circuit by using a low-cost amplifier IC which is BUF634. Through simulations, the functionality and performance of the system will be thoroughly assessed, ensuring its effectiveness in capturing lightning flashes.

The performance analysis of the lightning detection system was conducted by leveraging Pico-scope, Microsoft Excel, and MATLAB software. A dataset comprising 111 instances of lightning data was meticulously examined to categorize the types of lightning flashes captured in July 2023. The analysis specifically focused on distinguishing between the performances of the BUF634 and OPA633 components in terms of lightning flash detection accuracy. This validation process aimed to ensure the system's reliability in capturing real lightning events during a thunderstorm day.

To thoroughly assess the system's resilience, an extended two-month comparative study was carried out, meticulously examining the performance of the BUF634 against the OPA633 components. The focus of this performance evaluation specifically homed in on negative cloud-to-ground lightning flashes, considering the parameter of return stroke. The results, derived from a thorough analysis utilizing Pico-scope,

Microsoft Excel, and MATLAB software tools, provide valuable insights into the system's overall effectiveness. This comprehensive evaluation enables informed assessments of the lightning detection capabilities of the system, particularly shedding light on the relative performance of the BUF634 component throughout the designated two-month timeframe.

1.5 SIGNIFICANT OF THE PROJECT

Investing in lightning detection systems can improve understanding of weather patterns, enhance disaster preparedness, and support the development of climate-resilient communities. Low-cost lightning detection systems can play a crucial role in infrastructure resilience, public safety in urban areas, and early warning mechanisms. Technological innovations are needed to reduce costs while maintaining effective detection capabilities. Collaboration between governments, private sector organizations, and civil society is essential to successfully implement low-cost lightning detectors and develop sustainable partnerships. Governments can share knowledge, establish standards, and collaborate on funding. Partnerships with the private sector can drive technology transfer and innovation. These efforts can accelerate the adoption of low-cost systems and ensure their long-term viability.

1.6 THESIS ORGANIZATION

This thesis is structured into five chapters as follow:

Chapter 1 is an introduction. This Chapter discusses the background of the project and theoretical of lightning flashes. Problem statements are identified based on the

literature review and observations of the sensor used in high-cost system for lightning detection system. This is followed by an objective to be achieved throughout the study and scope of work which narrows down the area of the study and to complete the overall system. Lastly, state the significance of the project to ensure that the system achieves the sustainable development goals.

Chapter 2 is a background study. This chapter covers the basic theories regarding the research topic and the previous study from report and journal. The theoretical of lightning flashes, basic understanding of antenna, and previous project that used a low-cost system to detect lightning flashes will be shown in this chapter.

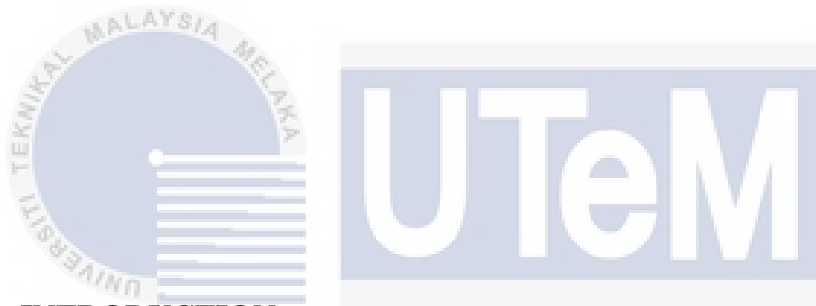
Chapter 3 is a methodology. This chapter explains the method selection to complete the whole system, which is design, simulation, testing, fabrication, calibration, measurement, and analysis. A flowchart diagram is an illustration of the process to complete the whole system and will be explained clearly step by step.

Chapter 4 is a result and discussion. This chapter will show the result obtained from the system, which is the electric field of lightning flashes signal, and system performance. All the measurements detail that obtained from the system will be shown in this chapter. This is followed by a discussion part to discuss all the information that relates to lightning flashes and performance.

Chapter 5 is a conclusion. This chapter is to summarize the findings and to conclude that the objective of the project was achieved. Lastly, give recommendations for future development to improve the overall system.

CHAPTER 2

BACKGROUND STUDY



2.1 INTRODUCTION

This chapter presents the previous study using a low-cost system to detect lightning. It aims to examine the existing research, methodologies, and technologies employed in the design and implementation of these systems. By critically analyzing the literature, can gain insights into the challenges and advancements in developing cost-effective lightning detection systems. This literature review will contribute to the field by consolidating the existing research and informing the design and development of an innovative low-cost lightning detection system. Through this project, aim to make lightning detection more accessible, affordable, and reliable, opening new possibilities for enhanced safety measures and improved decision-making in lightning-prone environments.

2.2 REVIEW ON LIGHTNING FLASHES

Lightning is a sudden, high-energy event that can cause significant damage to structures and infrastructure. They occur when there is a build-up of electrical charge in the atmosphere, which is then discharged through the air. Lightning can occur within a thunderstorm cloud, between cloud and cloud or between the cloud and the ground. The striking point of lightning on a tall structure is not always the top of the structure but sometimes it is the lower part of the structure. There are four type of CG lightning which is negative downward lightning, positive downward lightning, negative upward lightning, and positive upward lightning [12] [13] [14] as show in figure 2.1.

Figures 2.1 depict instances of downward lightning, while Figures 2.1(c) and (d) illustrate upward lightning phenomena. Downward lightning, which accounts for approximately 90% of CG flashes, is primarily initiated by negatively charged leaders moving downward as show in figure 2.1(a). In contrast, around 10% of CG lightning instances are initiated by positively charged leaders propagating downward as show in Figure 2.1(b). The remaining two types of lightning discharges shown in figures 2.1(c) and (d) are known as upward-initiated discharges, typically occurring from tall man-made structures, and referred to as GC lightning discharges. Figure 2.1(c) represents a positively charged upward lightning, which can induce a decrease in the negative charge of the cloud. Conversely, Figure 2.1(d) portrays a negatively charged upward lightning, capable of reducing the positive charge in the cloud. It is important to note that the term "upward" indicates the direction of the leader, while "negative" or "positive" denotes the transferred charge polarity from the cloud.

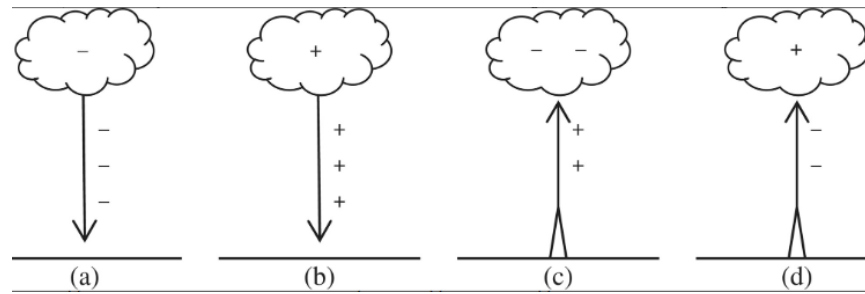


Figure 2.1: Type of cloud-to-ground lightning [12]

Positive lightning, sparked by downward leaders channeling positive charge to the ground, represents only about 10% of all CG strikes. Due to their rarity, positive strikes have been less explored than their negative counterparts. Understanding the charge dynamics in thunderclouds generating positive lightning, as well as the in-cloud processes initiating them, remains largely elusive. Specifically, electric field measurements suggest that positive strikes are preceded by significant in-cloud discharges lasting over 100 or 200ms. Positive lightning occurrences might be linked to severe weather phenomena like strong winds, large hail, and tornadoes.

Characteristics such as stroke frequency, continuing current, leader behavior, and branching differ notably between positive and negative lightning. Bipolar lightning, involving sequential discharge of positive and negative charges, can transfer positive charges to the ground but is not typically considered a major part of lightning activity, despite being potentially as common as positive strikes. Exploring different cloud charge configurations and scenarios that lead to positive lightning as shown in Figure 2.2. New data from Florida and existing literature, examining the role of in-cloud discharges in triggering positive lightning, subsequent strokes in established and newly formed channels, preliminary breakdown, and leader movement [15].

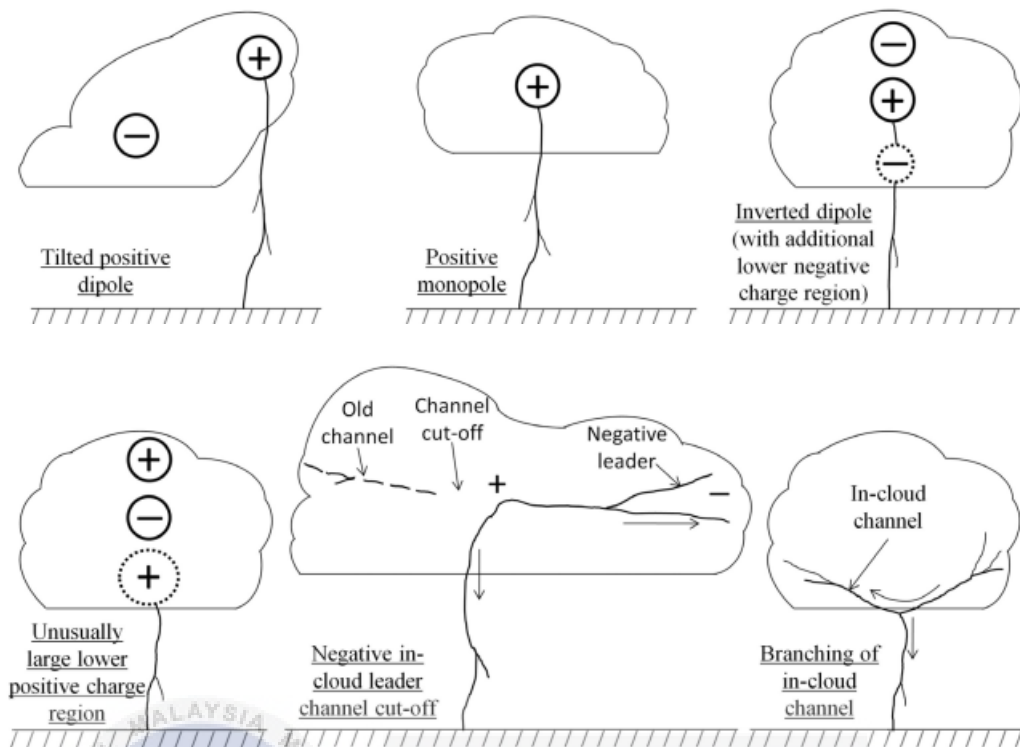


Figure 2.2: Conceptual cloud charge configurations and scenarios leading to production of downward positive lightning [15].

During upward drafts, minuscule ice particles within the cloud create friction, leading to a polarization process. Positive charges produced in this process move upward within the cloud while negative charges move downward. As the cloud expands, the electric potential difference between its upper positive and lower negative parts increases, inevitably resulting in electrostatic discharge reactions between these regions. When these discharges occur within the same cloud, they are termed IC discharges [16] [17], whereas those involving two or more clouds are termed IC or CC discharges. These types of discharges contribute to about 75% of global lightning events and do not involve contact with the Earth's surface. CG discharges, on the other hand, are the most impactful lightning events concerning human and terrestrial life on the Earth's surface [18].

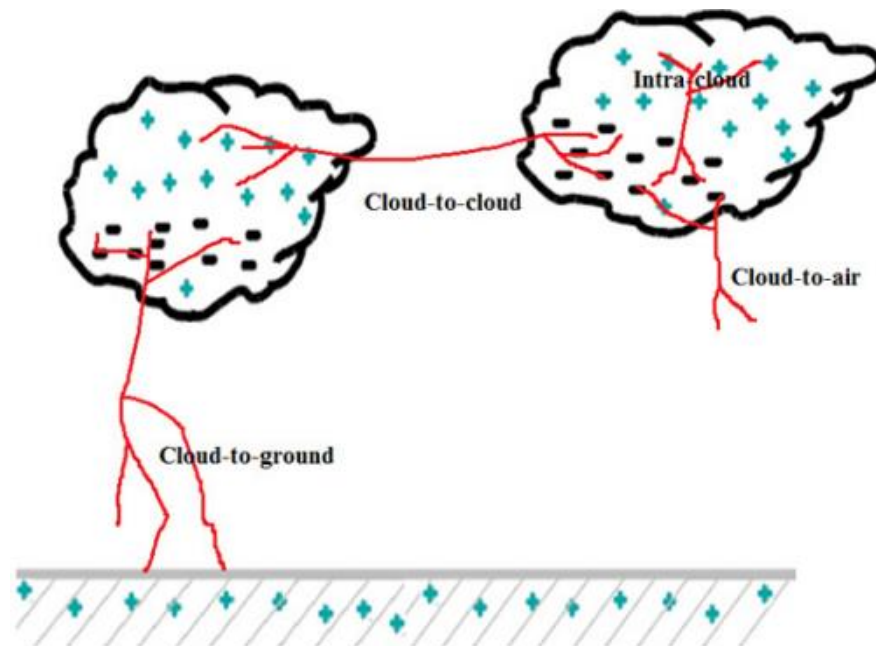


Figure 2.3: Different types of lightning discharge [18]

2.3 CHARACTERISTIC OF ANTENNA

The parallel flat-plate and vertical whip antennas were used to detect the vertical component of lightning electric field signals during thunderstorm days. Variations in the intensity of the atmospheric electric field result in corresponding changes between the top metallic plate of the antenna and the ground, regardless of whether a lengthy vertical-whip antenna pole or a parallel flat-plate antenna configuration is used. To prevent any interference from the horizontal electric field, the parallel plate antennas were positioned perpendicular to the electric field vector, or parallel to the ground. Lightning is the transfer of significant charge between two charged objects, it can appear between CC and CG. Lightning flashes produce wideband electromagnetic pulses ranging from a few Hz to several GHz.

Fast-electric field, 3 MHz radiation fields, and the time derivative of the electric field were measured using three separate parallel-plate antennas. A slow electric field

signal was observed using a vertical whip antenna. Each parallel-plate antenna consisted of two horizontal discs, with the top plate serving as the active plate and the other plate grounded. The antennas had approximate dimensions of 0.05 m insulator thickness, 1.5 m physical height, and 0.47 m diameter. Figure 2.4 illustrates the arrangement of these antennas, positioned adjacent to each other with a separation of 2 meters. The vertical-whip antenna comprised a lower metal rod, an upper metal rod (3.3 m in height), and an insulator separating the two rods. The lower metal rod was situated 2 meters above ground level, and a 0.05 m thick nylon insulator was used to isolate the top and bottom metal rods. The vertical-whip antenna was placed perpendicular to the parallel flat-plate antenna, maintaining a 2-meter distance between them. The antennas are situated 10 meters from the control room, where the recording devices are located. To mitigate unwanted reflections, matching resistors are incorporated at the oscilloscope input for the long coaxial cables. [19]



Figure 2.4: Parallel flat plate antenna [19]

Besides that, using a small-scale parallel plate antenna can measure the fast electric field signal. For lightning electric field measurement, a specific electronic circuit is used to measure an interest lightning electric field waveform. Figure 2.5 illustrates the proposed small-scale parallel plate antenna design, featuring a physical height of 0.555 m. The antenna comprises two circular aluminum plates positioned in parallel. The

upper plate has a diameter of 0.25 m, while the bottom plate has a diameter of 0.20 m. A gap of 0.03 m separates the two parallel plates, which is divided into three insulating layers made of Perspex, each with a diameter of 0.02 m. The main purpose of these insulating layers is to prevent direct contact between the conducting aluminum plates and to mitigate the occurrence of corona discharge between the plates.

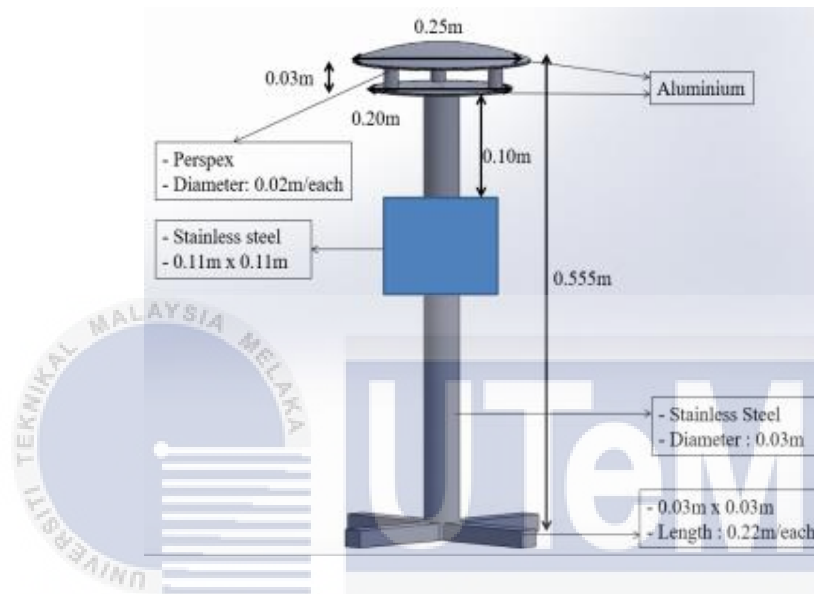


Figure 2.5: Small-scale parallel plate antenna [20]

As the electric field (E-Field) undergoes fluctuations during a thunderstorm, the induced charge on the antenna varies accordingly, resulting in the generation of current in the electric circuitry. On the other hand, field mills are specifically designed devices used to gauge the strength of the electric field on the Earth's surface. They can measure the combined effects of the static E-Field and the charge carried by clouds passing overhead. Typically, field mills comprise one or two electrodes that can rotate within an electrostatic field or be periodically exposed to the field through rotating vanes as shown in Figure 2.6.

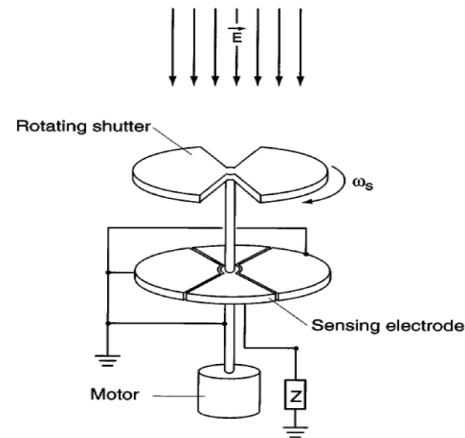


Figure 2.6: Vertical whip antenna [21]

The E-field associated with lightning can be measured using a flat metallic plate antenna. The E-field is quantified as the force experienced per unit charge, considering that the plate is positioned above the ground level. It is important to note that the E-field has a time-varying nature, and the wavelength of the field is significantly larger than the size of the metallic plate.

The measurement of the E-field involves monitoring the time-varying current that flows through the electric element connecting the metallic plate and the ground. However, the type of electric element used determines the nature of the measured current. It can be either directly proportional to the E-field or its derivative. In the case where a capacitance is employed as the electric element between the metallic plate and the ground to measure the voltage, integrating the current over time would allow for the determination of the E-field. The Electric Element Attached to the Antenna is shown in Figure 2.7.

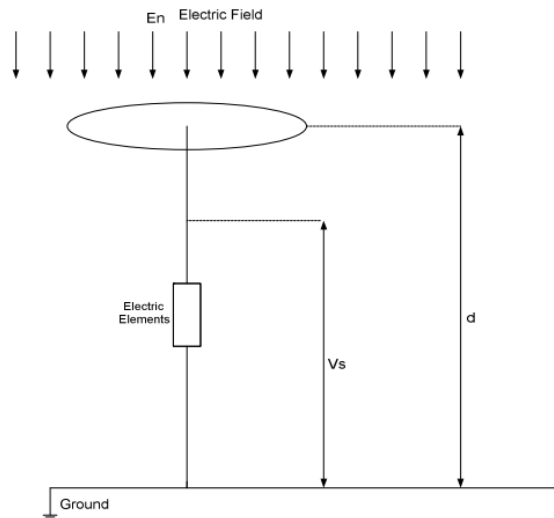


Figure 2.7: Electric element attached the antenna [21]

In Figure 2.8 show that E_n is the vertical component of the electric field, V_g is the voltage through the antenna, C_g is the capacitance of the parallel plate antenna, C_c is the capacitance of the 60cm length of coaxial cable which is functioned to connect antenna and the electric circuit. R_1 is the input resistor between the coaxial cable and electronic circuit. C_1 is the capacitor used as an electric element to measure the E-field by measuring the changes in the voltage V_g of the parallel plate. Capacitor C_1 was shunted by high value resistor R_2 that controls the decay time constant $C_1 \cdot R_2$.

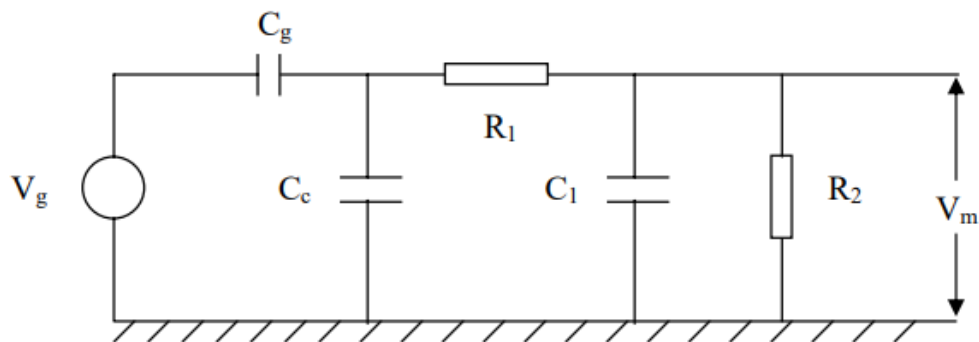


Figure 2.8: Electric element circuit of the system [21]

2.4 REVIEW ON SPECIFICATION OF BUFFER AMPLIFIER CIRCUIT WITH THE RESULT OBTAINED.

2.4.1 LH0033 High-Speed Buffer Amplifier

The parallel plate antenna was connected to the high-speed buffer amplifier which is LH0033 to deliver the signal from parallel plate antenna to the recording unit. The schematic diagram of buffer amplifier circuit is shown in Figure 2.9 and the measured negative lightning return stroke was obtained by referring to the pico-scope as shown in Figure 2.10. A total of 115 negative return strokes have been observed from the 205 lightning signals. An example of the measured negative return stroke signal with the negative stroke's zooming, which the signal represents up to the zero crossings [20].

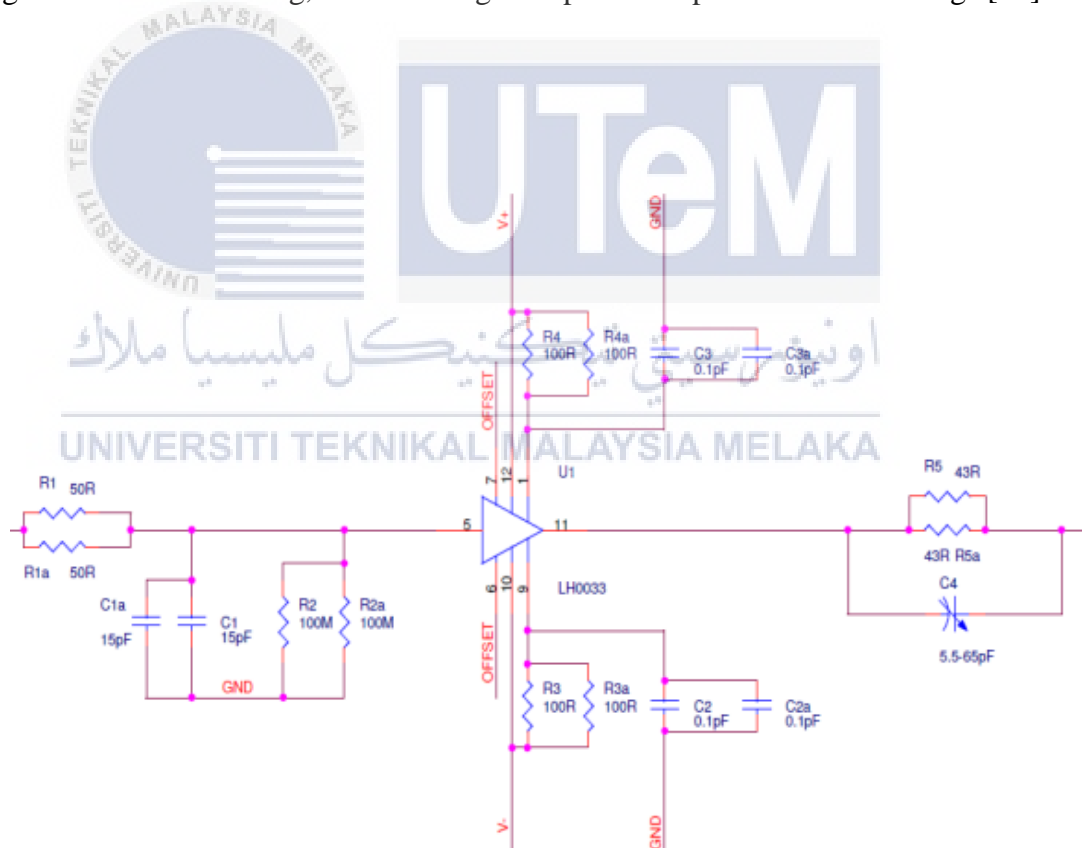


Figure 2.9: Schematic diagram of buffer amplifier circuit [20]

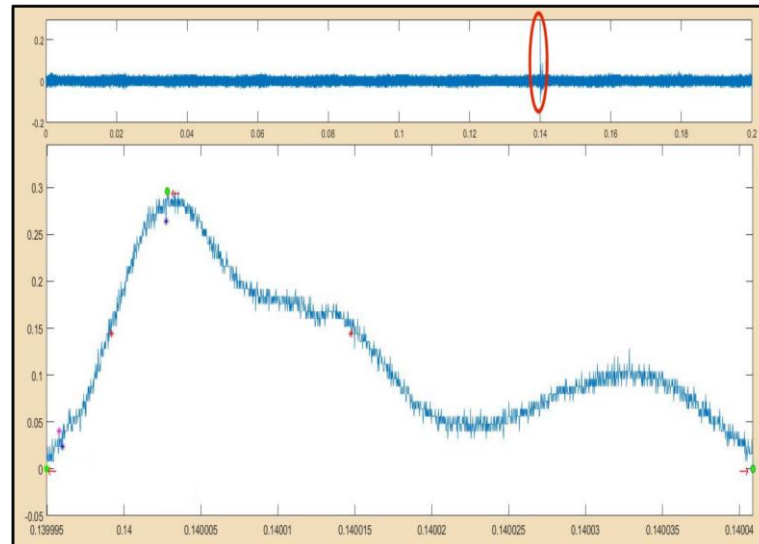


Figure 2.10: Measured negative lightning return stroke [20]

Besides that, Adhikari et al also show that +CG lightning can be measured by referring the positive return stroke on the signal capture by using LH0033 high-speed buffer amplifier as show in Figure 2.11 while -CG lightning strike can be determined on the negative return stroke. Most of the positive ground flashes were found to have single strokes. However, some of the negative ground flashes consisted of two or more return strokes. A new electronic circuit alternative for the measurement of lightning generated electric fields was proposed, calibrated, and validated.

133 positive ground flashes were recorded on different thunderstorm days. Most of the positive ground flashes were characterized by single stroke flashes whereas the occurrence of the multiple stroke flashes was relatively very rare. In Figure 2.12 show the example of stroke flash where scope 1 is the total overall of flash obtained. Then scope 2 is the zoomed signature of the first return stroke of the four-stroke positive flash. For scope 3 depicts the expanded form of second return stroke and scope 4 depicts the third and fourth return strokes of the same flash.

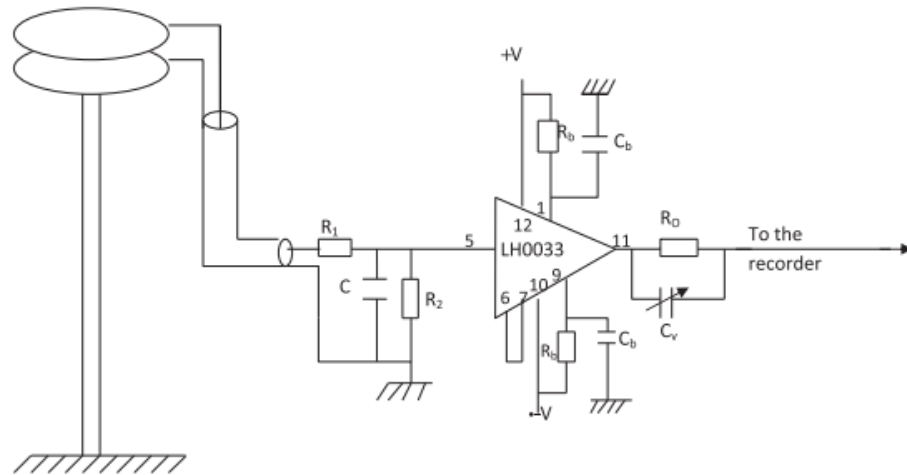


Figure 2.11: Connection of parallel plate antenna and buffer circuit [22]

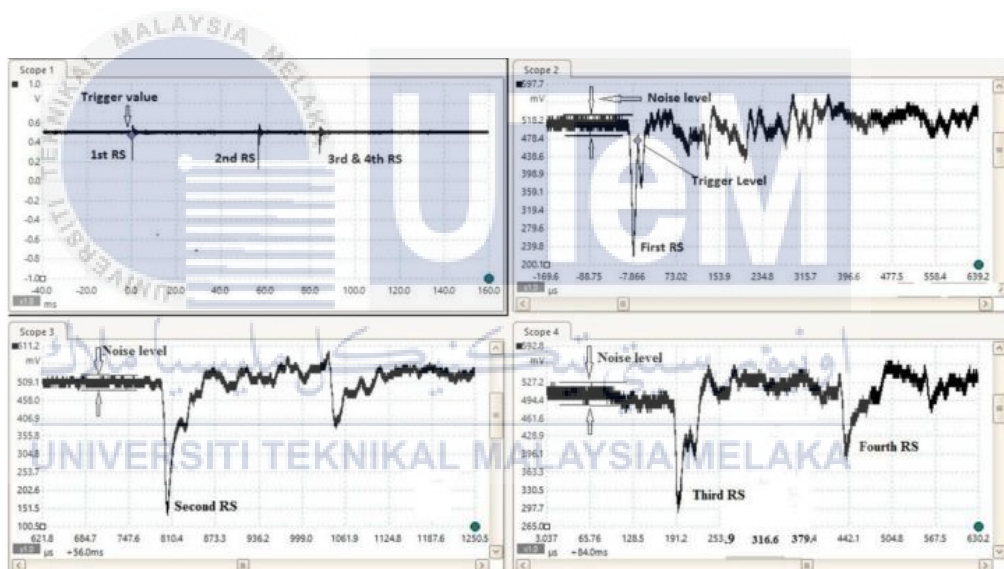


Figure 2.12: Example of stroke flash recorded [22]

Figure 2.13 illustrates an instance of a return stroke characterized by double peaks. Each peak represents the surge of residual charge along the ionized channel. It was observed that the preliminary breakdown (PB) pulses associated with positive ground flashes exhibited less prominence compared to the corresponding PB pulses of

negative regional flashes. Consequently, only a limited number of positive flashes displayed distinct PB pulses. Figure 2.14 provides an example of a PB pulse.

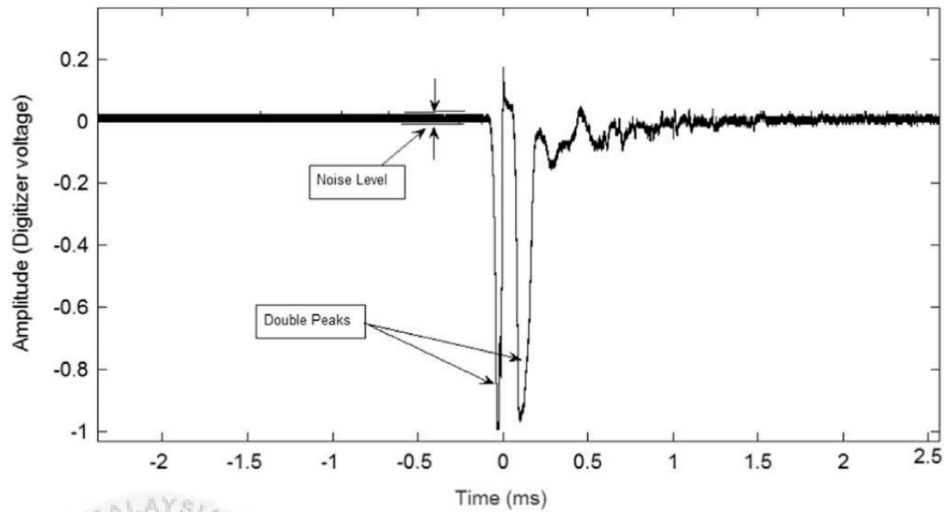


Figure 2.13: Example of return stroke with double peaks [22]

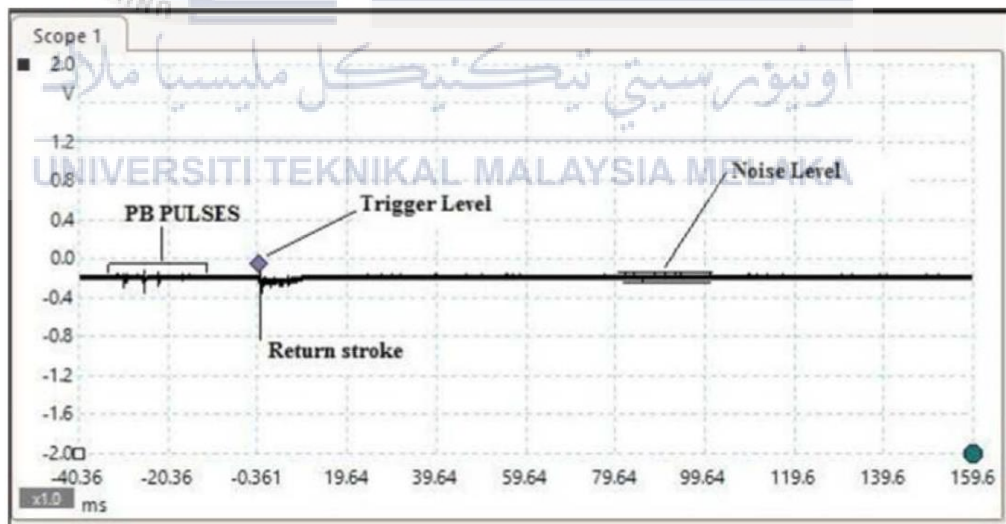


Figure 2.14: A flash consist of preliminary breakdown pulse [22]

The stepped leader preceding positive ground flashes exhibited less prominence in comparison to their negative counterparts. Consequently, only a limited number of positive flashes displayed a distinct stepped leader. Figure 2.15 illustrates an example of a flash with a stepped leader followed by a positive return stroke [22].

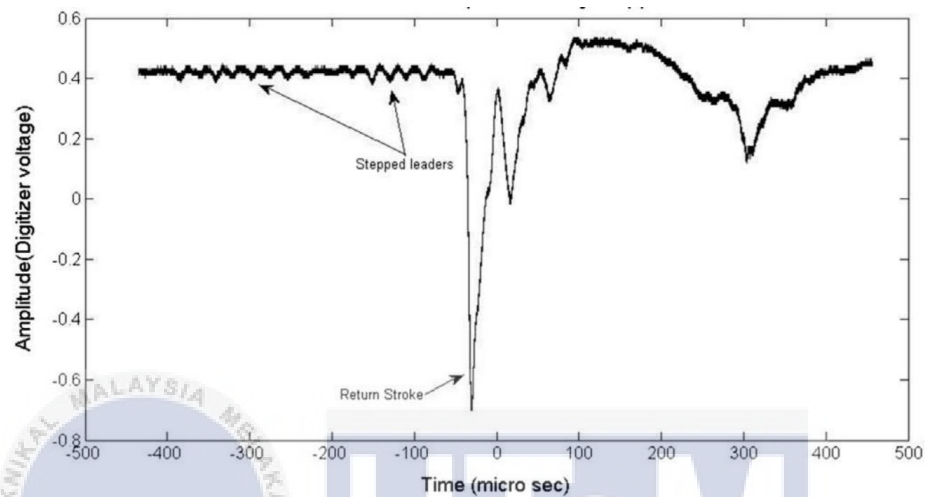


Figure 2.15: Example of positive return stroke [22]

2.4.2 – OPA633 High-Speed Buffer Amplifier

Edirisinghe et al and Baharin et al using a high-speed buffer amplifier to capture the lightning. High-speed buffer amplifier is used to measure lightning generated vertical electrical fields. A high-speed Buffer Amplifier circuit was constructed with a buffer amplifier IC OPA633 to measure the vertical electric fields generated by lightning. Resistor and capacitor were used to design a high-speed buffer amplifier as shown in Figure 2.16. By employing a high-speed buffer amplifier, the antenna's high impedance is separated, and sufficient power is provided to transmit the signal from the antenna to the recording unit via the coaxial cable. The connection between antenna, electric element and recording unit is shown in Figure 2.17. According to the frequency response of the circuit, it is seen that the circuit is suitable for recording

lightning generated electric fields up to MHz region. The amplifier is capable of safely driving capacitive loads up to $0.01\mu\text{F}$, allowing for the use of up to a 100m coaxial cable between the amplifier and the recording unit to avoid any distortions [23] [24].

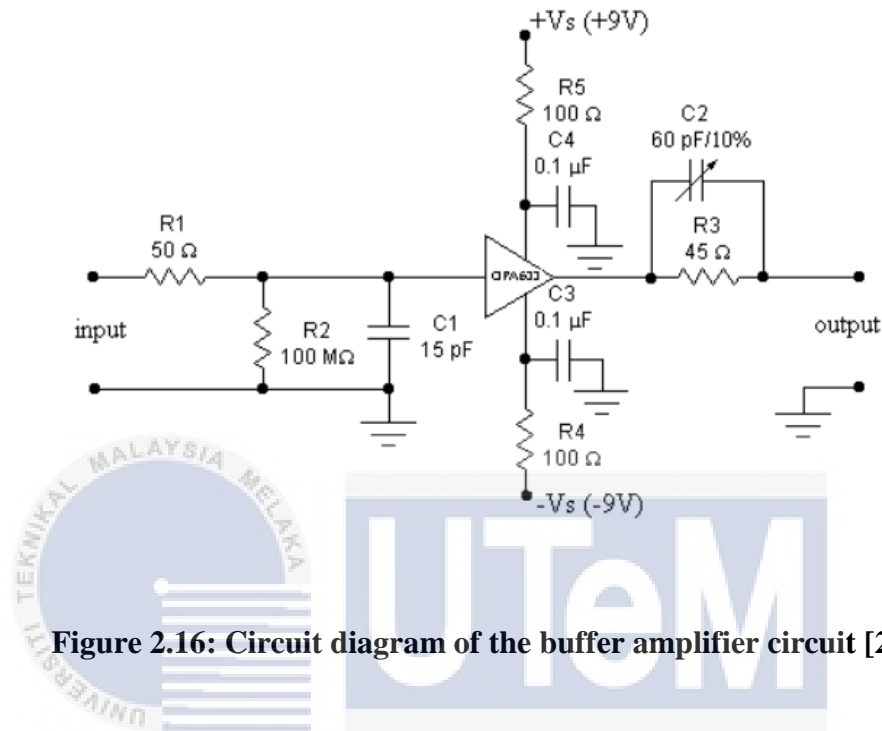


Figure 2.16: Circuit diagram of the buffer amplifier circuit [23]

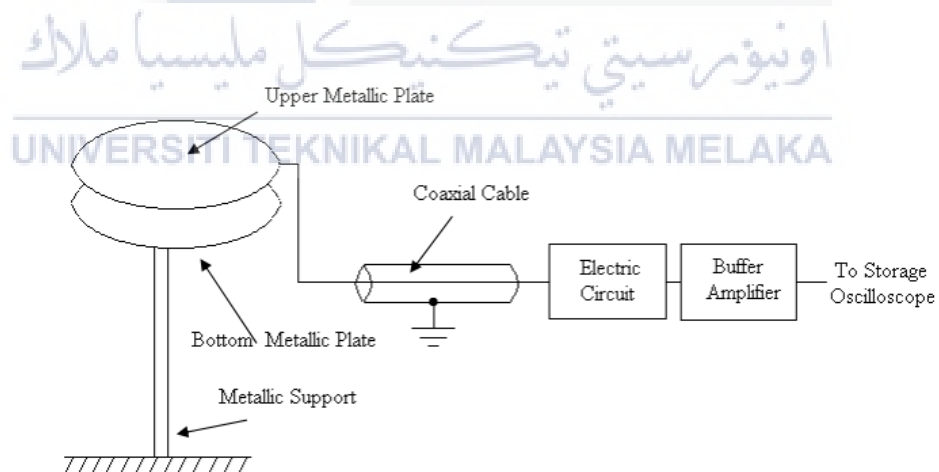


Figure 2.17: Block diagram of the electric field measuring system [23]

2.4.3 BUF602 High-Speed Buffer Amplifier

Rojas et al. was shown that the electronic circuit based on the buffer amplifier circuit can replace the classic electric field measuring system as shown in Figure 2.18. It is also suitable for recording electric field changes of both near and far fields. Due to its decay time constant, the electronic circuit can record the typical electrostatic components of the electric fields in the range of less than 50 km. However, if the physical height of the parallel-plate antenna is different to 1.25 m. Figure 2.19 illustrates a representative example of the characteristic pattern observed in a recorded -CG lightning flash using the proposed measuring system. This pattern includes the presence of PB pulse trains, followed by the first return stroke and six subsequent return strokes [25].

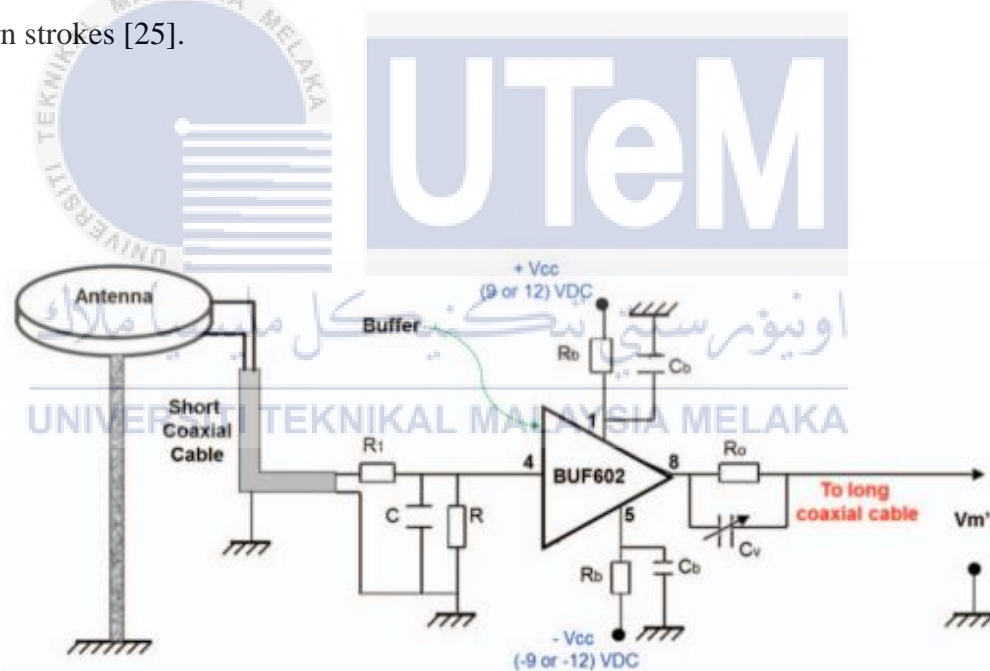


Figure 2.18: Buffer amplifier circuit [25]

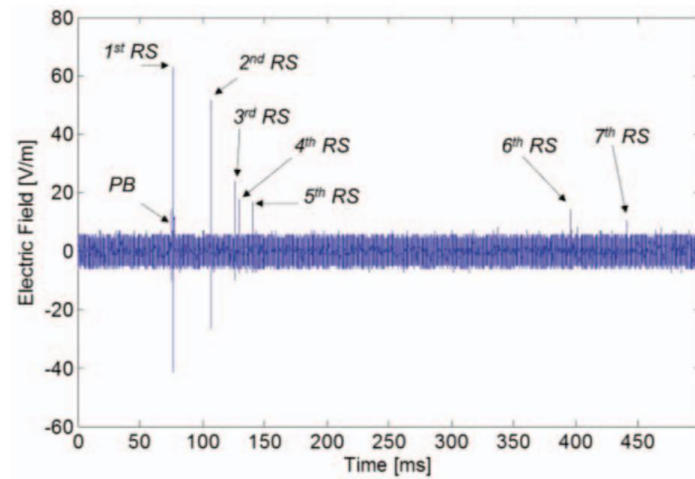


Figure 2.19: Negative cloud-to-ground lightning flash [25]

2.4.4 BUF634 High-Speed Buffer Amplifier

In electronic circuit design, using an open loop buffer circuit which is BUF634. Buffer circuit contains a unity gain and additionally makes an adequate impedance coupling due to its positions between the antenna and the oscilloscope, by means of passive elements with the aim of minimize reflections or distortions in the captured signals. The components used in the circuit design are resistor, capacitor, and BUF634. The 50 Ω coaxial cable can be used as a transmission line. The measurement system of an electric field is shown in Figure 2.20.

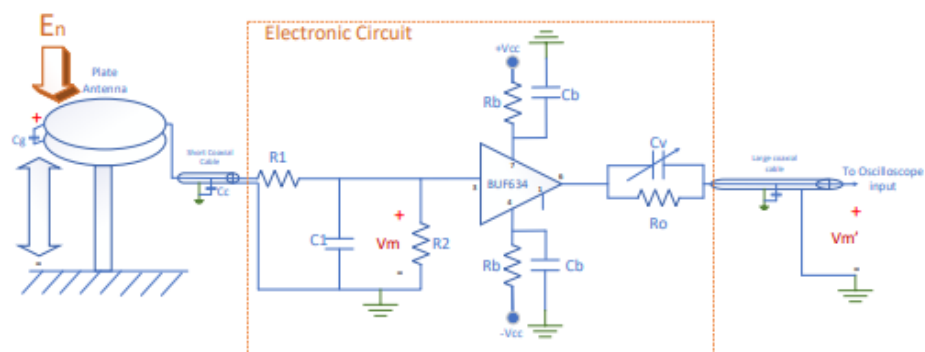


Figure 2.20: Measurement system of an electric field [26]

By using Measurement system as shown in previous Figure 2.20, The system able to detect negative and positive lightning strike. For negative lightning flashes characteristic, an initial peak with a fast front followed by a descend ramp, then the first zero crossing and finally some polarity changes are presented, especially for events with distance longer than 100km, the longer the distance, the higher the oscillations. For positive lightning flashes characteristic, positive waveforms have slower front time than negative, and the waveform of positive return strokes is like negative with some special characteristics [26].

Besides that, Ramle et al show that measure the parameters such as amplitude and risetime of the electric fields generated by lightning using the amplifier-oscilloscope method, it is crucial to design an amplifier circuit that can provide precise measurements. This can be achieved by utilizing a high-speed buffer amplifier circuit [27] as shown in Figure 2.21. The primary function of the buffer amplifier is to isolate the high impedance of the antenna and provide sufficient power to transmit the signal from the antenna to the recording unit through the coaxial cable. Capacitor C_b resistor R_b is functioned to protect the circuit from damages due to excessive currents [21].

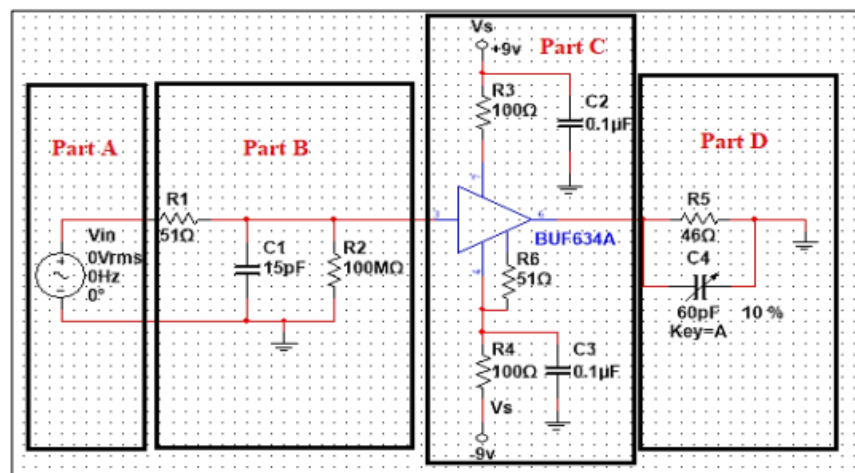


Figure 2.21: Electronic circuit connected to the antenna [21]

2.5 PARAMETER OF CLOUD-TO-GROUND LIGHTNING FLASHES

Within the categorization of CG lightning, two primary types exist: -CG and +CG lightning. -CG lightning involves the transfer of negative charge from the cloud to the ground and constitutes approximately 90% of CG strokes. Given that the negative charge center of clouds typically resides at a lower altitude than the positive charge center, the stroke channels for -CG lightning usually span 5-8 km. It's the flow of current through these kilometer-long channels that generates radiation with wavelengths on the kilometer scale (3-30 kHz), categorized as very low frequency. Figure 2.22 show the example of cloud-to-ground lightning flashes [28].

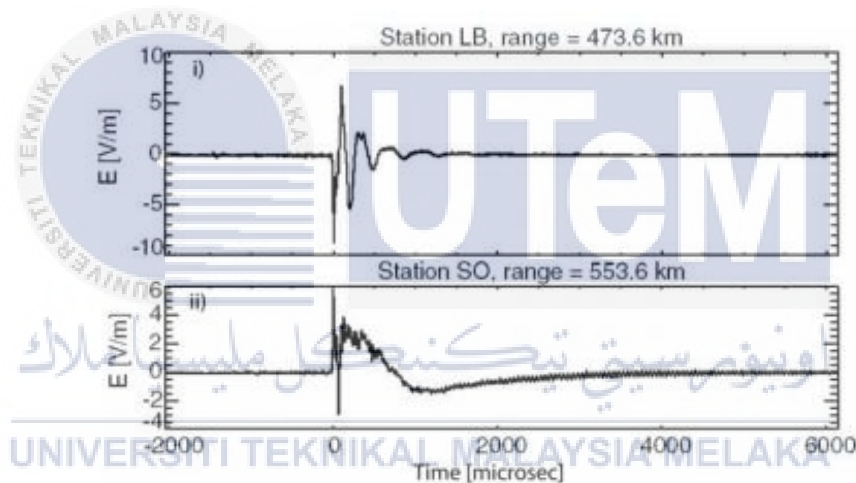


Figure 2.22: Example of cloud-to-ground lightning flashes [28]

Figure 2.23(a) illustrates a return stroke from a +CG flash, while Figure 2.23(b) depicts a return stroke from a -CG flash [29]. During the initial ascent of the return stroke, two characteristics were identified: a gradual rise known as the slow front, followed by a relatively rapid climb to the peak called the fast transition. Typically, the transition point between these phases is approximately 50% from the start of the return stroke to its peak for the first instance, while subsequent return strokes display

a breakpoint around 20% [30]. In the third observation, the zero-to-peak rise time refers to the duration from the start of the return stroke to its maximum peak. The fourth parameter observed is the zero-crossing time, indicating the moment the radiation field crosses the zero line. Finally, the pulse duration of the return stroke, defined as the time taken for the radiation field of the return stroke to complete one cycle, was also measured [31].

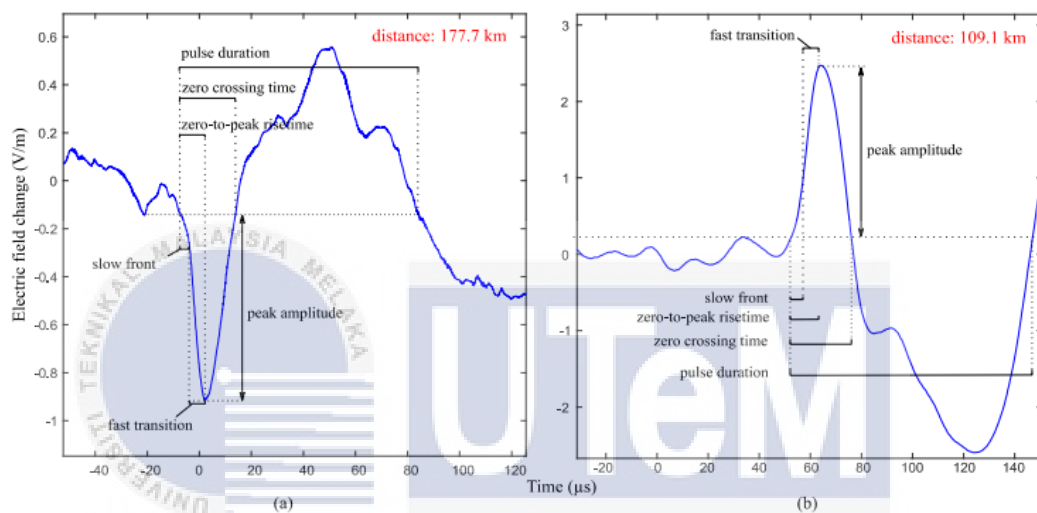


Figure 2.23: The characteristics of a return stroke for (a) a positive cloud-to-ground and (b) a negative cloud-to-ground flash [31]

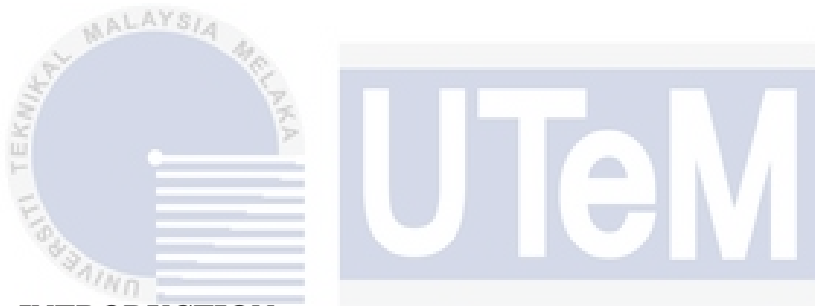
Yusop et al show that CG flashes contain +CG and -CG flashes. Most of the positive +CG flashes were single-stroke or two-stroke while -CG flashes were multiple strokes. All first return strokes were produced by initial PB. The important parameters that need to be observed are flash multiplicity and inter-stroke interval. Flash duration and first-to-subsequent stroke field peak ratio. The average of multiplicity and maximum strokes for +CG flashes is less than -CG flashes [32]. The main positive charge center is screened from the ground by the main negative charge center and this pattern is influenced by the shape and size of the thunderstorm.

2.6 SUMMARY

This section presents a comprehensive literature review encompassing various aspects pertinent to lightning flashes, antenna characteristics, high-speed buffer amplifier design, and parameters associated with CG lightning flashes. Initially, lightning flashes are categorized into two types: CG and IC lightning flashes. Within CG lightning flashes, two distinct characteristics exist (negative and positive) polarity. The significance of antenna characteristics for accurate lightning detection is notable. Previous studies highlight three primary types of antennas: parallel plate antenna, small-scale parallel plate antenna, and vertical whip antenna. Each antenna type possesses unique characteristics tailored to specific applications. For seamless transmission of lightning signals to the recording unit, the integration of a high-speed buffer amplifier into the system is essential. Noteworthy buffer amplifier options include LH0033, OPA633, BUF602, and BUF634. LH0033 functions optimally within the frequency range of 300Hz to 1MHz, detecting CG lightning. OPA633 extends the detection capability to both CG and IC lightning within a frequency range of up to 1MHz. BUF602 detects -CG lightning in the frequency range of 100Hz to 12MHz, while BUF634 captures CG and IC lightning signals within the 1Hz to 10MHz frequency range. Lastly, a comprehensive overview of parameters defining C lightning flashes encompasses peak amplitude, pulse duration time, zero-crossing time, zero-to-peak rise time, slow front, fast transition, and the occurrence of single or multiple return strokes. The interval between two distinct return strokes is termed as the inter-stroke period. This compilation of studies and findings contributes significantly to the understanding and effective detection of lightning flashes, antenna selection based on specific requirements, and the critical role of high-speed buffer amplifiers in lightning signal processing.

CHAPTER 3

METHODOLOGY



3.1 INTRODUCTION

This chapter describes the methodology of low-cost lightning detection systems by explaining in detail about the method of research, hardware development, set up lightning detection system, and lightning data collection. The process of designing a low-cost lightning detection system and analysis type of lightning flashes will be clearly shown and explained in this chapter.

3.2 METHOD OF RESEARCH

Figure 3.1 shows the process of designing a lightning detection system. In this process, all component and circuit designs will be determined and designed, including the type of components used and their values. After that, the circuit will be designed using Proteus software. All the components and circuits will be designed, and the functionality will be tested to manipulate the signal using an oscilloscope. In the simulation process, the completed circuit will be tested by increasing the frequency of the input signal and observing the signal characteristics on the oscilloscope. If the signal obtained is incorrect, the circuit will be troubleshooted and redesigned. If the signal obtained is correct, the process will proceed to the fabrication process.

Next, the lightning detection system will be designed and simulated by assembling several components: antenna, coaxial cable, buffer circuit, Pico Scope, and laptop. After that, the system will be calibrated to detect lightning using a spark device, which will work as small lightning strikes. If the system fails to detect the lightning generated by the spark device, it will be troubleshooted and calibrated. If the system can detect lightning, it will be proceeded to set up a lightning detection system at the top of the FTKEK building and collect real lightning data. Finally, the collected data will be analyzed by identifying the type and characteristics of lightning flashes.

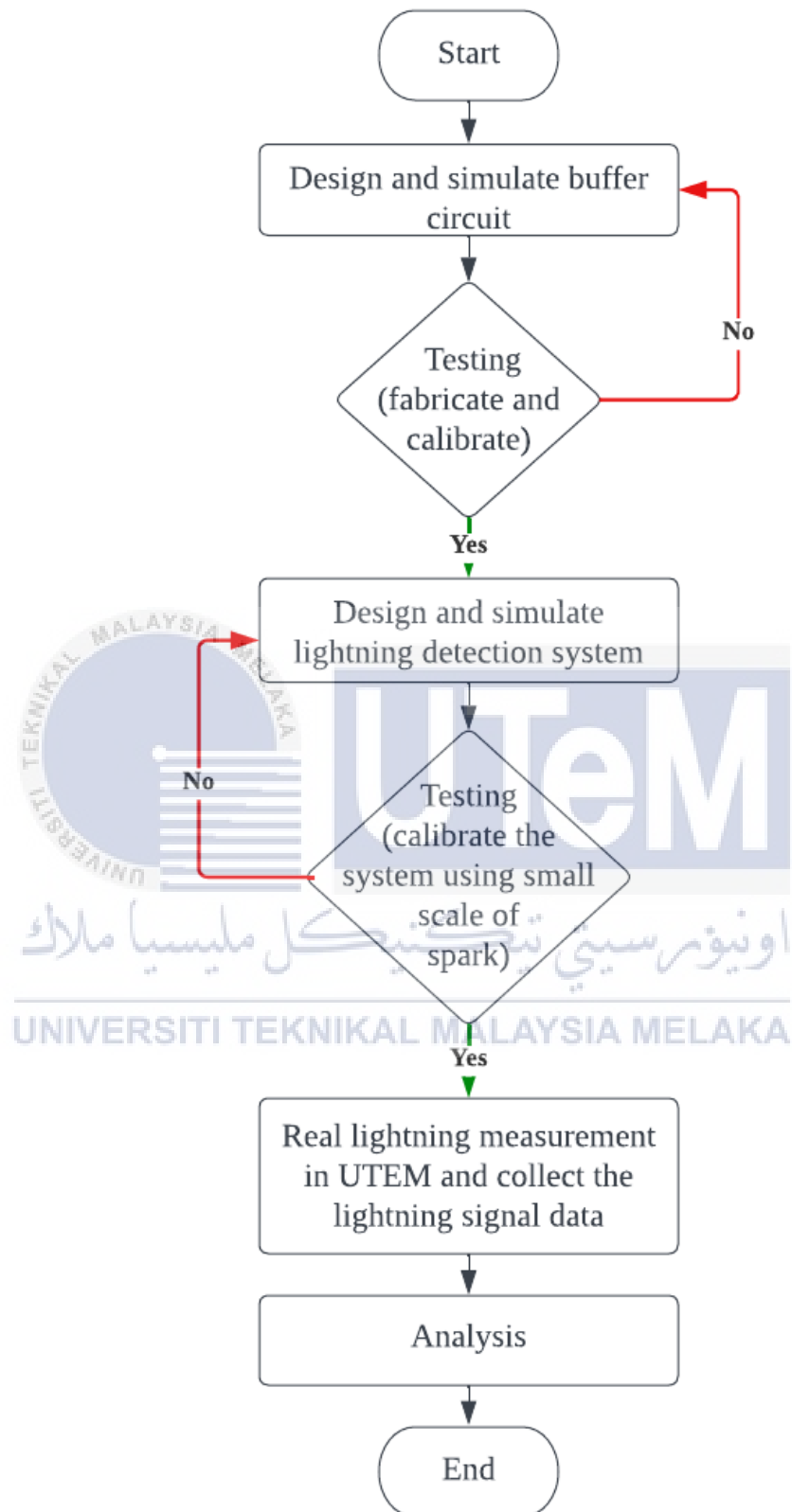


Figure 3.1: Flow chart of designing the low-cost lightning detection system.

3.3 HARDWARE DEVELOPMENT

3.3.1 Designing buffer circuit.

The investigation of lightning flashes, which comprises pulses lasting from milliseconds to microseconds, requires a fast field circuit capable of capturing segments of the lightning discharge within these specified time frames. The precision of the electrical setup is vital for accurately capturing the amplitude and rise time, crucial parameters in measuring the swift electric field. Achieving accurate measurements necessitates an appropriate decay period in the resistor-capacitor (RC) circuit within the fast field circuit.

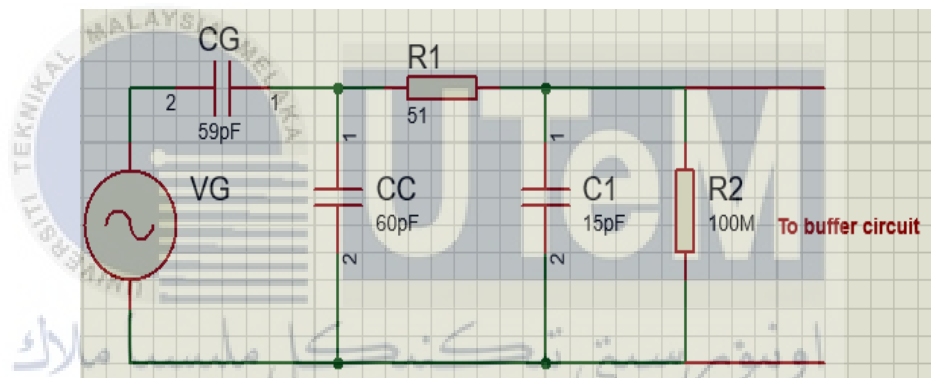


Figure 3.2: Resistor-capacitor circuit

C_g represents the capacitance of the parallel plate antenna, measuring 59pF in this paper. Additionally, C_c signifies the capacitance of the 60cm coaxial cable connecting the parallel plate antenna to the electrical circuit, which amounts to 60pF. C_1 , functioning as the capacitor for electric field measurement by monitoring voltage changes (V_g) across the parallel plates, was specifically a 15pF capacitor. This capacitor, C_1 , was coupled with a high-value resistor, R_2 , to regulate the decay time constant, $C_1.R_2$.

The decay time constant,

$$\tau = (C_g + C_c + C_1) \times R_2 \quad (1)$$

$$\tau = (59p + 60p + 15p) \times 100M \quad (2)$$

$$\tau = 13.4ms \quad (3)$$

To design and simulate a buffer circuit, the initial step involves determining the circuit's requirements and specifications. In this case, the BUF634 buffer IC was chosen as a cost-effective replacement for the OPA633. The circuit is designed to operate using negative and positive 12V DC power supplies. The buffer circuit was constructed by arranging and interconnecting the designated components, with values set according to the design specifications. The resistors (R1, R2, R3, R4, and R5) were set to 51 Ω , 100M Ω , 47 Ω , 100 Ω , and 100 Ω respectively, while capacitors (C1, C2, and C3) were set to 15pF, 0.1 μ F, and 0.1 μ F respectively. Fast Field (FF) buffer circuit operating frequency is between 1Hz to 10MHz with decay time constant 13ms. The use of 15pF of C1 is to maintain the decay time constant 13.4ms. The use of 15pF of C1 is to maintain the decay time constant 13.4ms. The fast field buffer circuit design is depicted in Figure 3.3. By comparing the input signal on channel 1 with the output signal on channel 2, showcased in Figure 3.4, the simulation results were analyzed to detect any discrepancies or deviations from the intended specifications. Adjustments to component values were then made to optimize the amplifier circuit's performance based on the findings from the simulation analysis.

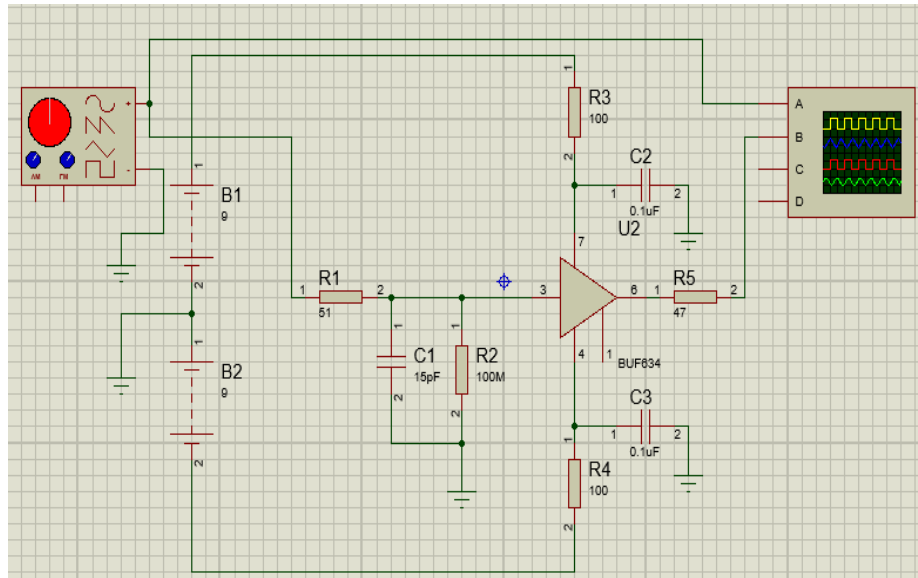


Figure 3.3: Circuit design of Fast Field buffer circuit

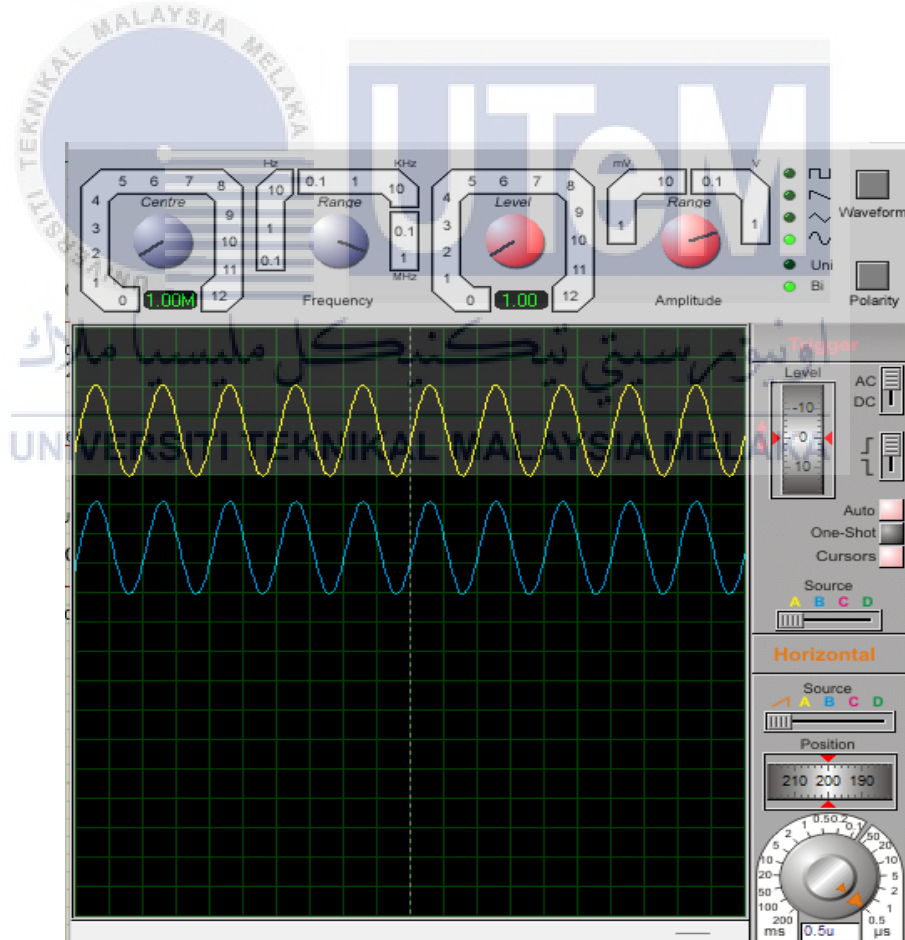


Figure 3.4: Comparison input frequency and output frequency for buffer circuit

3.3.2 Fabricate buffer circuit.

This section involves the fabrication process for buffer circuits, encompassing the procurement of essential components and materials necessary for constructing the circuit. This includes obtaining the Printed Circuit Board (PCB), BUF634 buffer IC, resistors, capacitors, connectors, and other necessary elements aligned with the circuit design. The circuit's layout on the PCB is created, mirroring the depiction in Figure 3.5. Components are accurately positioned within their designated areas, establishing vital connections between them. Ensure proper spacing, clearances, and trace routing to avoid any short circuits or interference. Replace all the components in the PCB layout and connect them to each other according to the circuit design.

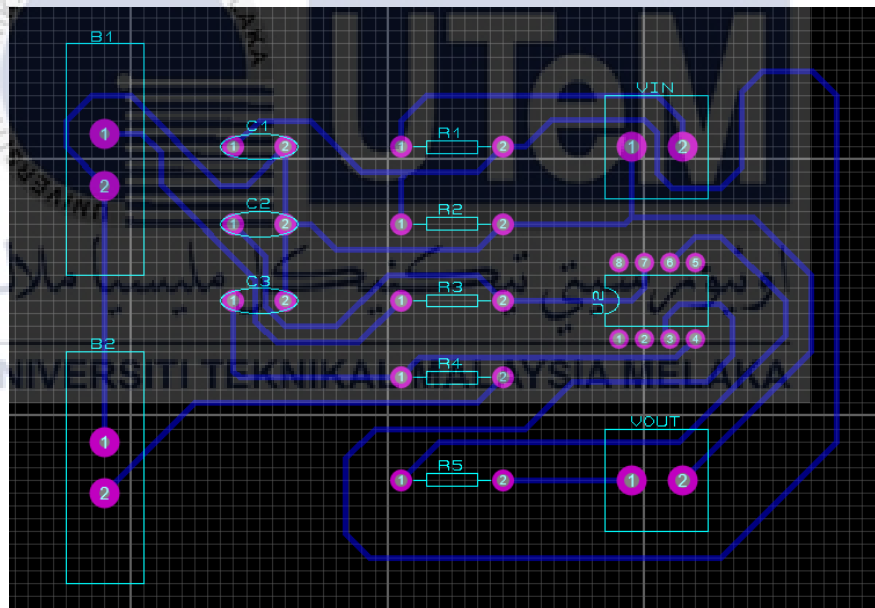


Figure 3.5: Printed circuit board layout for buffer circuit

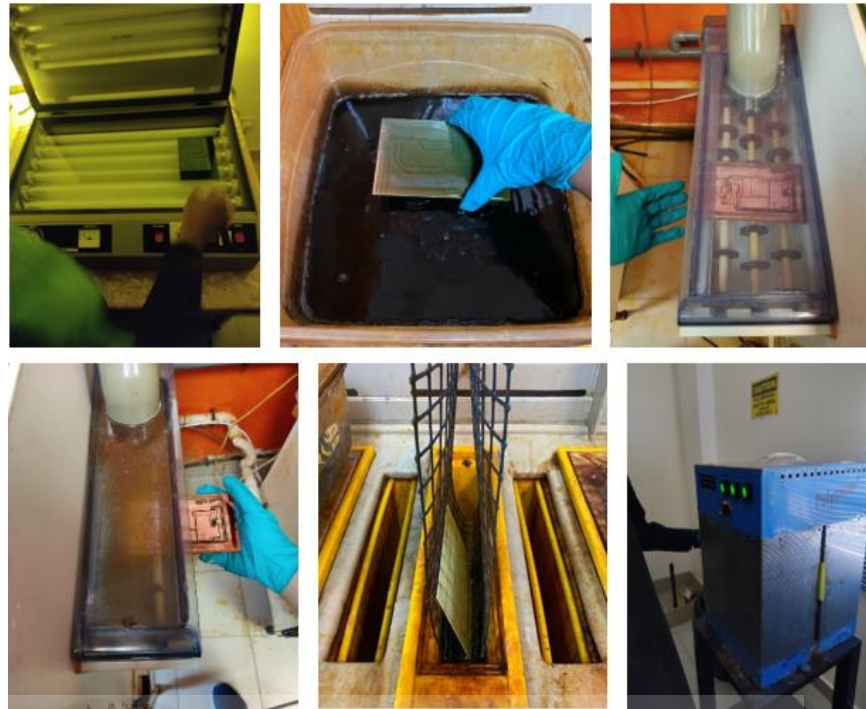


Figure 3.6: Fabrication process to remove unwanted copper.



Figure 3.7: Completed fabrication process.

Figure 3.8 illustrates the placement of components on the PCB in alignment with the designated design layout. Ensure the correct orientation and alignment of each component before securing them onto the PCB. Using a soldering iron and solder wire, the components are soldered onto the board, adhering to proper soldering techniques to establish reliable connections while avoiding solder bridges or cold solder joints. A thorough inspection is conducted to scrutinize the solder joints and connections for any potential defects or issues. Subsequently, electrical tests, such as continuity checks and voltage measurements, are performed to verify the circuit's functionality. This systematic approach ensures the integrity and proper functioning of the fabricated circuit.



Figure 3.8: Placing the component on printed circuit board.

3.3.3 Calibrate buffer circuit.

Figure 3.9 shows the calibration process of the FF buffer circuit. To ensure precise operation, the FF buffer circuit undergoes a calibration process. The function generator from Pico scope connects to channel 1 on Pico scope and to the input signal

at the FF buffer circuit. Then, the output signal connects to channel 2 on Pico scope. The signal obtained is evaluated by observing the signal on channel 1 and channel 2. Evaluation involves comparing signals from both channels, and equivalence validates the system's functionality. The system was tested by allowing 1MHz frequency at the input of FF buffer circuit and measured the output signal. The result of calibration showed that the output signal is equivalent to the input frequency as shown in Figure 3.10. If necessary, Fine-tuning and optimizing the FF buffer circuit's performance involves adjusting component values, modifying circuit parameters, or adding compensation circuits to enhance performance or address any calibration discrepancies. The importance of selecting materials efficiently, minimizing waste, and promoting sustainable practices in the fabrication process will encourage proper handling of components and materials, reducing environmental impact.

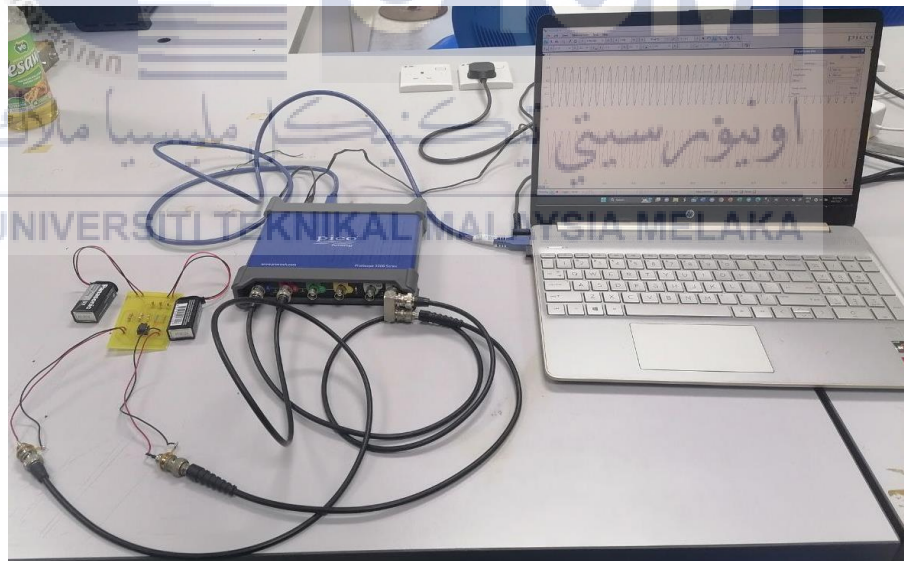


Figure 3.9: Calibration process to evaluate the functionality of buffer circuit.

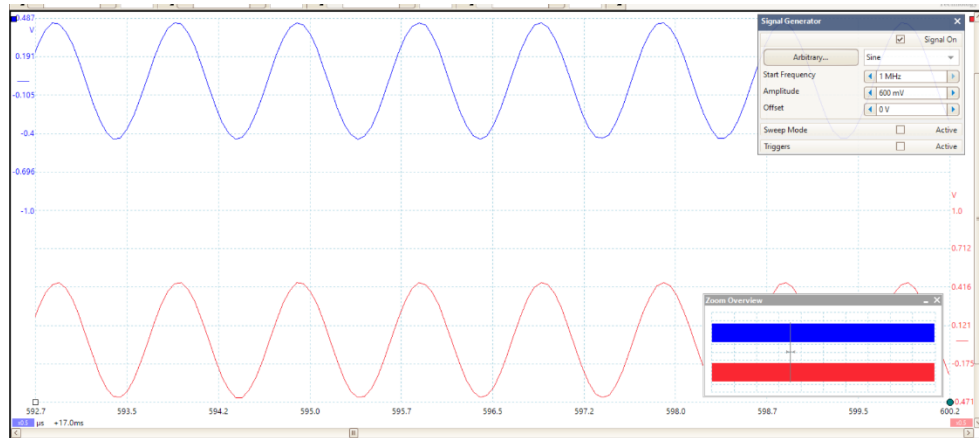


Figure 3.10: Signal calibration at 1MHz frequency

3.4 SET UP OF LIGHTNING DETECTION SYSTEM

3.4.1 Designing lightning detection system.

The process of designing the lightning detection system involved assembling several components: antenna, coaxial cable, FF buffer circuit, Pico Scope, and laptop. The chosen antenna for lightning detection was a parallel plate antenna constructed using metallic material, depicted in Figure 3.11. The antenna used in this design had a capacitance of 59pF. To establish connectivity, the designed antenna was linked to the buffer circuit through a short 60cm coaxial cable with a 50Ohm impedance. The capacitance of the coaxial cable is 60pF. Subsequently, the buffer circuit was connected to the Pico Scope via a longer coaxial cable, and the Pico Scope was interfaced with the laptop. The configuration and arrangement of all these elements are illustrated in Figure 3.12. Upon triggering by lightning flashes, the system collected and stored all the data within the Pico Scope software for further analysis and evaluation.

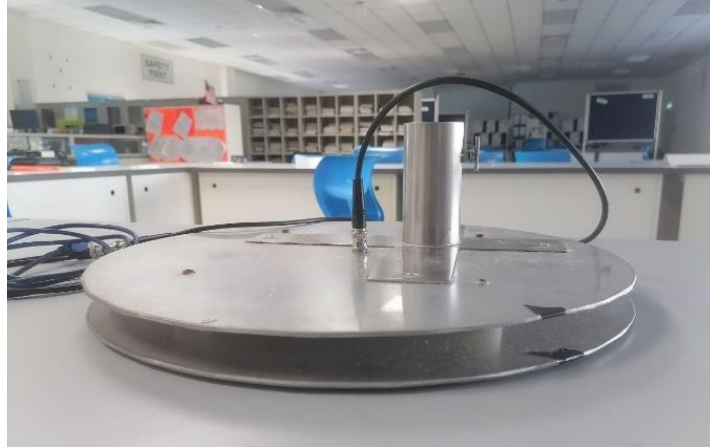


Figure 3.11: Parallel plate antenna



Figure 3.12: Completed system arrangement

3.4.2 Calibrate lightning detection system using small-scale sparks.

The system calibration involved using a small-scale spark to ensure its capability to detect actual lightning flashes. This calibration step utilized an electric mosquito killer to generate these smaller sparks, simulating lightning flashes for system testing. Electric mosquito killer, serving as a source of scaled lightning flashes, was positioned near the antenna. The signals captured by the antenna were transmitted via a short

coaxial cable to the buffer circuit. From there, the signals were directed to the recording unit and displayed on a laptop for observation and analysis. The complete calibration process is visually represented in Figure 3.13. The characteristic signal obtained from these small-scale lightning flashes is illustrated in Figure 3.14. This signal served as a reference point for evaluating and confirming the system's ability to detect and capture lightning-related signals accurately.

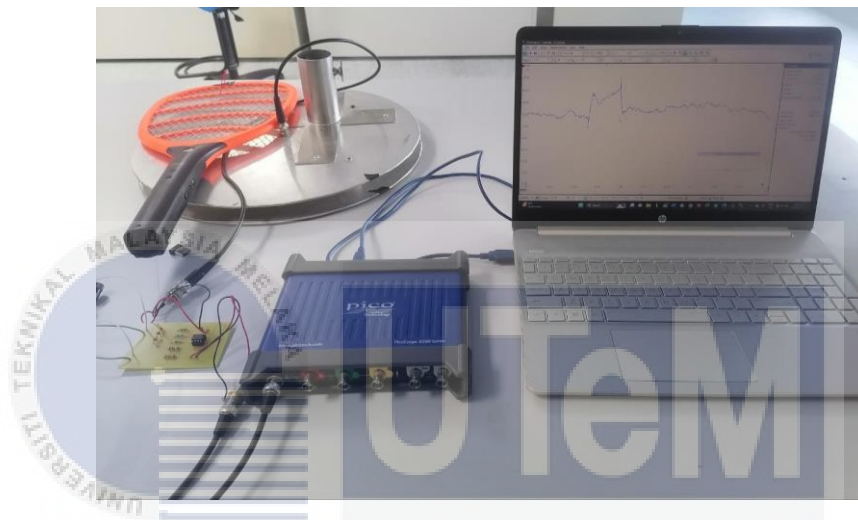


Figure 3.13: Calibration using small-scale of spark.

UNIVERSITI TEKNIKAL MALAYSIA MELAKA

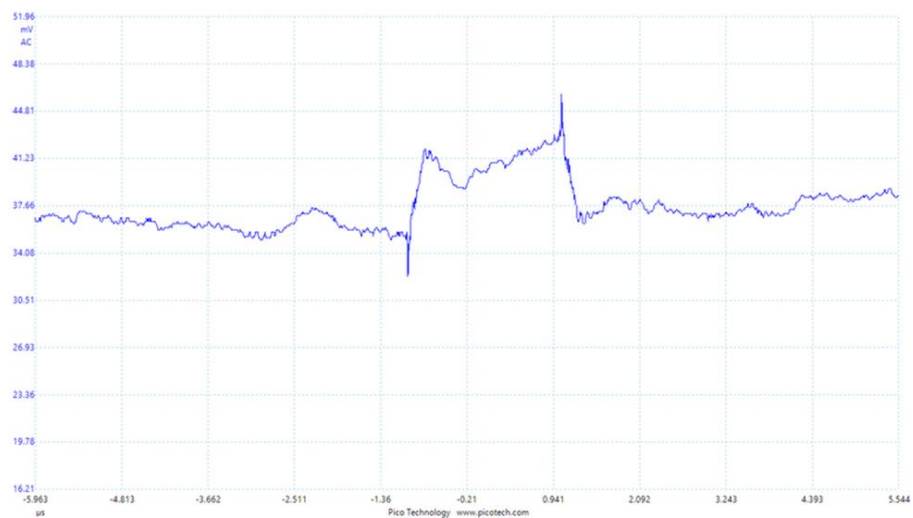


Figure 3.14: Small-scale lightning flashes

3.4.3 Lightning Measurement Setup in UTEM

This section illustrates the installation setup of a comprehensive lightning detection system at the UTEM building, emphasizing key considerations such as accessibility, unobstructed exposure to the open sky, and the absence of significant barriers that might impede detection accuracy. The setup entails the meticulous installation of a lightning detection system comprising an antenna, buffer circuit, and associated equipment. Each component was methodically positioned and configured to ensure optimal functionality and accurate lightning detection. Strategic placement of lightning detection system across the rooftop was executed to maximize coverage area. Factors such as the field of view, elevation angles, and line of sight were carefully evaluated to enhance the system's detection capabilities. This placement aimed to optimize the system's ability to capture lightning signals effectively. The location of this system installation is detailed in Figure 3.15, showcasing the precise positioning of components on the building rooftop. This setup was designed with thorough consideration of various environmental and technical factors to enable precise and comprehensive lightning detection.



Figure 3.15: Installation setup for Fast Field buffer circuit and antenna

3.5 LIGHTNING DATA COLLECTION

3.5.1 Identification types of lightning.

This section involves identifying the types of lightning signals based on the recorded data. 60 -CG flashes were identified on July 11, 2023, between 01:32:00 and 08:30:00. Each of the CG flash return strokes were observed based on its characteristic parameters, such as peak amplitude, pulse duration, zero crossing time, zero-to-peak rise time, slow front, and fast transition. The number of return strokes and the value of inter-stroke between the two return strokes were also measured. Not all -CG flashes have more than one return stroke. Of the total recorded 60 -CG flashes, 54 were single return stroke flashes, four were two subsequent return stroke flashes, and two were three subsequent return stroke flashes. A total of 60 -CG return strokes were located, although the others could not be found because of noise that contaminated the electromagnetic waveforms.

Figure 3.16 shows an example of a return stroke of a -CG flash parameter. The type of CG flashes is identified by referring to the rising part of the return stroke, which goes positive or negative. If the rising part of the return stroke is positive, it is known as -CG; otherwise, if the rising part of the return stroke goes negative, it is known as +CG. This happens because of the atmospheric sign convention. The first parameter is peak amplitude, which is measured from the bottom to the maximum amplitude. The initial rising part of the return stroke consists of two factors: the slow front and fast transition. The slow front is characterized by slow-rising segments, while the fast transition occurs during the rise to the peak, also known as fast transition. Normally, the first return stroke's breakpoint is around 50% from the stroke's beginning to its peak, whereas the succeeding return strokes have a breakpoint of 20%.

Regarding the next observation, the time interval from the beginning of the return stroke to the point at which the return stroke reaches its maximum peak is known as the zero-to-peak rise time. The next parameter is the zero-crossing time, which is the moment at which the radiation field crosses the zero line. The last parameter of the return stroke is the pulse duration, which is the amount of time the radiation field of the stroke ends a cycle. Additionally, the number of return strokes was measured by identifying the repeated return stroke after a single return stroke. The distance between two return strokes is known as inter-stroke, as shown in Figure 3.17.

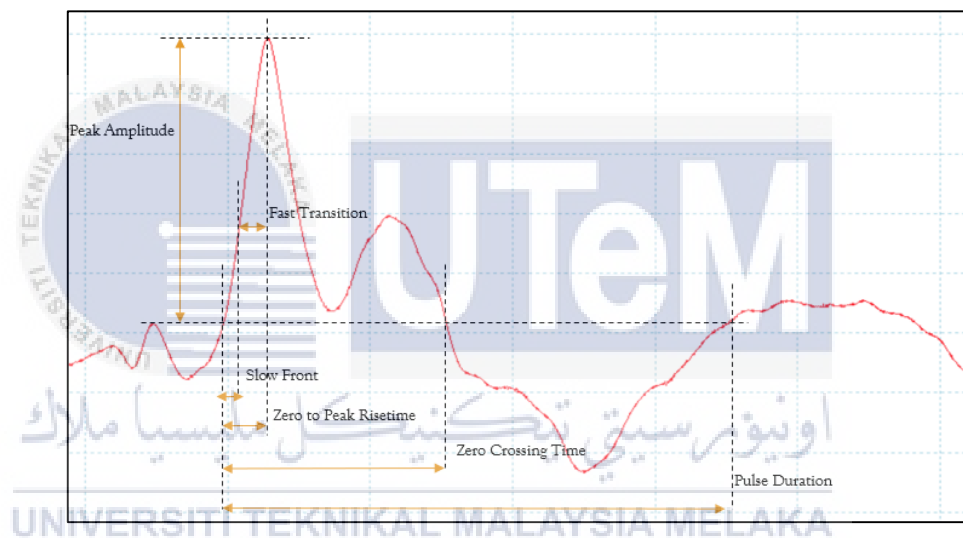


Figure 3.16: The parameter of negative cloud-to-ground lightning flash.

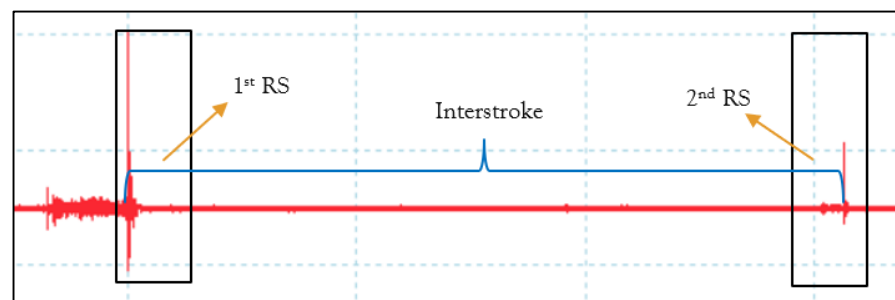


Figure 3.17: The parameter of multiple return stroke negative cloud-to-ground lightning flash.

Validate the results obtained through the analysis by comparing them with the existing system. Verification helps to ensure the accuracy and validity of the analyzed signal data. Summarize the characteristics and types of lightning observed and highlight any significant findings or observations. By evaluating the performance and effectiveness of lightning detection systems and analyzing lightning events, researchers and scientists contribute to enhancing our understanding of climate patterns and their potential impact on ecosystems and human activities. This knowledge can help in developing strategies to mitigate and adapt to climate change.

3.5.2 Data collection of lightning flashes

The process commenced by initiating the data collection phase, enabling the lightning detection system to continuously monitor atmospheric conditions for any lightning activity. Ensuring the proper functioning of data loggers, they were configured to reliably record and store the collected data. Specifically, two Fast Field measurements were taken, Fast Field 1 (FF1) from the existing system using OPA633 linked to channel A (Blue), and Fast Field 2 (FF2) from the current system using BUF634 linked to channel B (Red). The monitoring of lightning signals was illustrated in Figure 3.18. After a month-long period of continuous data collection, the recorded data from the data loggers was retrieved. This analysis focused on identifying distinct lightning signals, waveform patterns, and time intervals to isolate and classify lightning events based on their unique characteristics. The findings were collected and save at Microsoft excel to record all the data obtained during the thunderstorm event on 11 July 2023. The illustration of recorded data is shown in Figure 3.19.

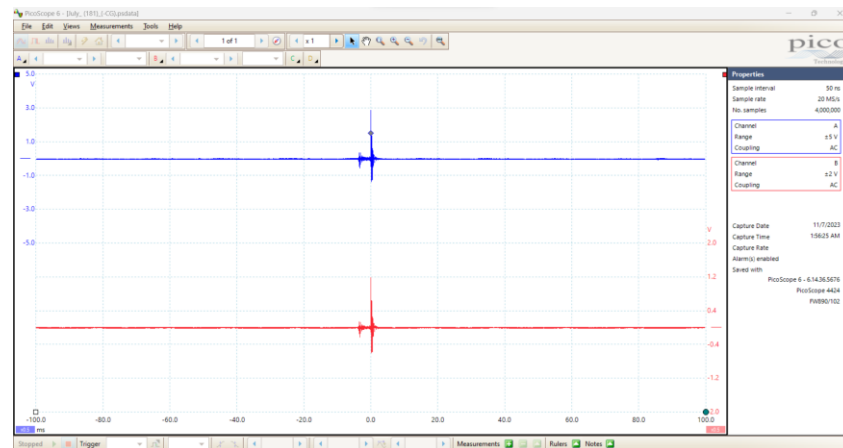


Figure 3.18: Monitoring lightning signal on 11 July 2023

Name	Type	Peak Amplitude (V)	Pulse Duration (µs)	Zero Crossing time (µs)	Zero-to-Peak Rise Time (µs)	Slow Front (µs)	Fast Transition (µs)	Return Stroke
July_(181)	Negative CG	2.646	161.8	39.63	13.7	7.152	6.548	1
July_(183)	Negative CG	1.7	36.09	25.12	4.365	1.218	3.147	1
July_(205)	Negative CG	1.434	39.48	28.49	4.887	1.673	3.214	1
July_(209)	Negative CG	1.504	101.05	25.13	4.523	1.44	3.083	1
July_(218)	Negative CG	1.28	54.77	27.16	4.833	2.092	2.741	1
July_(245)	Negative CG	2.226	44.14	21.62	9.957	6.818	3.139	1
July_(269)	Negative CG	1.652	26.02	22.9	6.338	3.444	2.894	1

a)

Name	Type	Peak Amplitude (V)	Pulse Duration (µs)	Zero Crossing time (µs)	Zero-to-Peak Rise Time (µs)	Slow Front (µs)	Fast Transition (µs)	Return Stroke
July_(181)	Negative CG	1.098	163.3	41.43	14.99	5.985	9.005	1
July_(183)	Negative CG	0.62	34.74	28.74	5.149	1.447	3.702	1
July_(205)	Negative CG	0.582	38.62	29.62	5.21	2.306	2.904	1
July_(209)	Negative CG	0.625	100.7	24.81	4.379	1.338	3.041	1
July_(218)	Negative CG	0.582	56.32	31.95	5.757	2.662	3.095	1
July_(245)	Negative CG	0.92	43.44	21.72	10.54	6.388	4.152	1
July_(269)	Negative CG	0.617	93.47	39.44	6.21	2.833	3.377	1

b)

Figure 3.19: Example of recorded lightning data on 11 July 2023 for (a) existing system (OPA633) and (b) current system (BUF634)

The Malaysian Meteorological Services recorded numerous lightning and thunderstorm occurrences, averaging around 200 days of thunder per year [33]. The results obtained showed that as many as 111 data points of lightning flashes were detected at the top of the FTKEK building using the low-cost lightning detection system. These lightning flashes were detected within a small radius of topical

thunderstorms in Malacca, Malaysia. The entire dataset has been analyzed and categorized into several types of lightning, namely -CG and IC. The identification of the flash type was based on the recorded fast electric field change. The recorded data includes 60 -CG and 51 IC lightning flashes as shown in Figure 3.20. The separated data comprises the selected data with a strong flash signal.

Signals from the parallel plate antenna and the electronic circuit were fed into a Pico-Scope using a 50-ohm coaxial cable properly terminated to avoid reflections. The Pico-Scope operated with a sampling time of 50 ns and a 100ms full observation window. The analysis focused on the -CG lightning flashes by measuring the flash characteristic parameters. Additionally, most of the -CG flashes were found to have single strokes; however, some of the -CG flashes consisted of two or more return strokes. Out of the total recorded 60 -CG flashes, 54 were single return stroke flashes, four consisted of two subsequent return stroke flashes, and two had three subsequent return stroke flashes. Figure 3.21 illustrates the number of strokes -CG flashes.

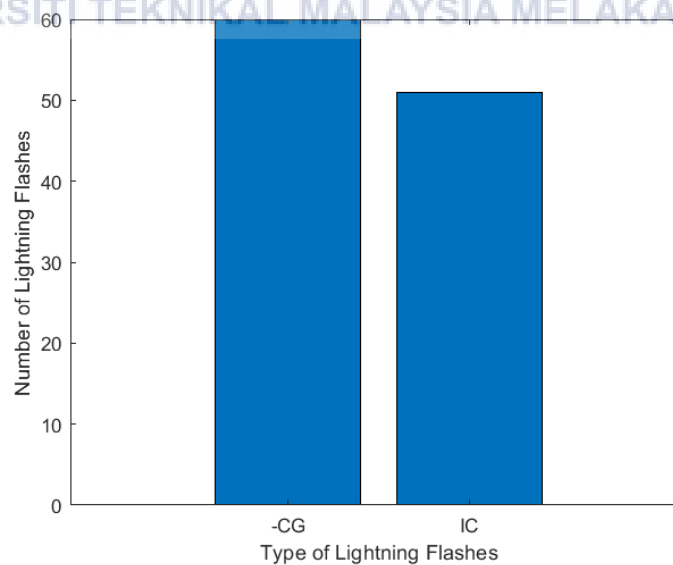


Figure 3.20: Number of recorder lightning flashes for negative cloud-to-ground and intra-cloud flashes

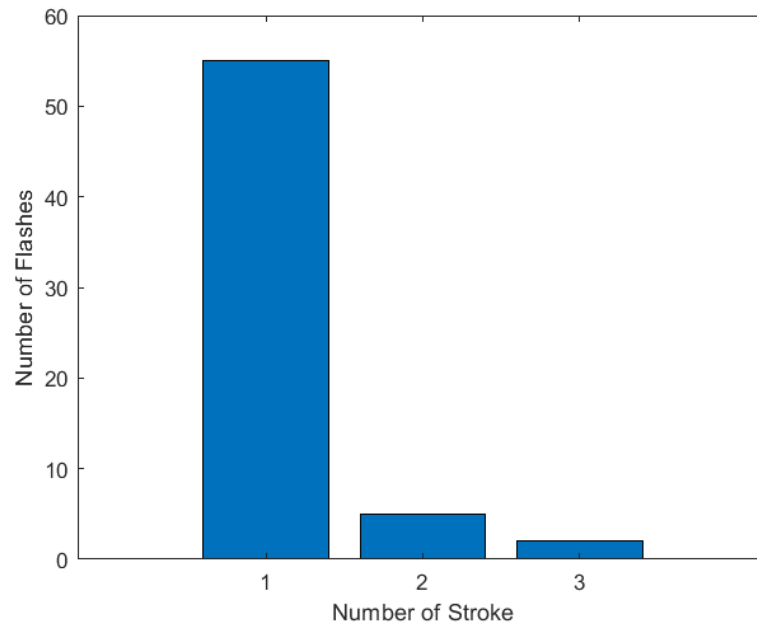


Figure 3.21: Distribution of the number of strokes per flash for negative cloud-to-ground flashes

3.6 SUMMARY

This chapter provides a comprehensive overview of the methodology employed in designing a low-cost lightning detection system. It details the step process involved in methodology of research, developing hardware, setting up the lightning detection infrastructure, and collecting lightning data. The emphasis lies in elucidating the intricacies of designing an economical lightning detection system, outlining the methodologies, hardware components, setup configurations, and calibration procedures crucial for accurate lightning detection. Additionally, the chapter delves into the analysis techniques used to interpret different types of lightning flashes, offering a clear and thorough explanation of the data analysis process.

CHAPTER 4

RESULTS AND DISCUSSION



4.1 INTRODUCTION

This chapter will present the result and discussion derived from the system, including the signal of lightning flash signals and an evaluation of the system's performance. Detailed lightning data obtained from the system will be thoroughly documented in this chapter. Subsequently, there will be a discussion section dedicated to exploring all the information pertaining to lightning flashes and system performance.

4.2 CHARACTERISTIC OF CLOUD-TO-GROUND LIGHTNING FLASHES

4.2.1 Negative cloud-to-ground flashes

Figure 4.1 shows that the characteristic of a return stroke was captured on July 11, 2023, from 01:32:00 until 08:30:00. The result shows that there are three different characteristics of negative -CG flashes, which are a single return stroke, two return strokes, and three return strokes. Each flash has its own signal form; by referring to Figure 4.1(a), there is a process seen at the beginning that is called the initial breakdown pulse or preliminary breakdown pulse, and the process is followed by a stepped leader and a return stroke. In Figure 4.1(b), the process was the same as in Figure 4.1(a), but the signal has two repeated return strokes that is called a -CG with two subsequent return strokes. In Figure 4.1(c), it was shown that there are three repeated return strokes that are called as -CG with three subsequent return strokes.

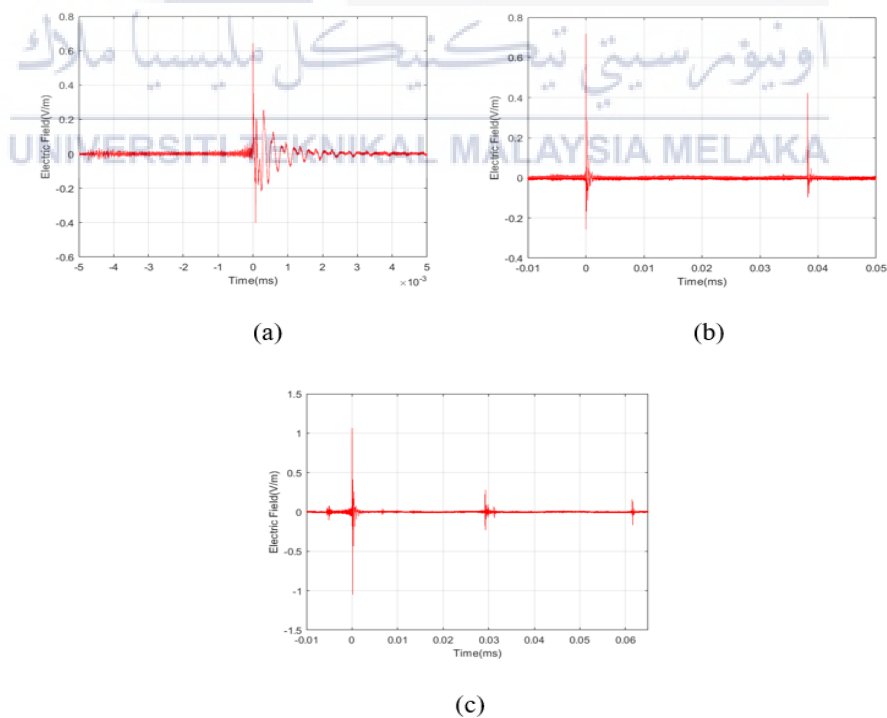


Figure 4.1: The characteristic of a return stroke for (a) negative cloud-to-ground flashes with single stroke, (b) negative cloud-to-ground flashes with two return strokes, and (c) negative cloud-to-ground with three return strokes.

4.2.2 Comparison negative cloud-to-ground lightning flashes between Fast Field 1 and Fast Field 2

The results of FF1 and FF2, as shown in Figure 4.2, 4.3, and 4.4, were captured at the same time by assigning FF1 to channel A and FF2 to channel B. The Pico-scope allows two channels (Channel A and Channel B) to be displayed simultaneously. Channel A generated the blue signal, whereas Channel B generated the red signal. The blue and red signals are from the same event of lightning, as they have identical shapes. Meanwhile, the circuit design was different between the two channels. The difference is that FF1 uses OPA633 to create a buffer circuit, while FF2 uses BUF634. Channel A will be used as a reference to identify the accuracy of the detected lightning flash. Figure 4.2 shows the difference between FF1 and FF2 for a -CG flash with a single return stroke. Figure 4.3 shows the difference between FF1 and FF2 for -CG flash with two subsequent return strokes, and Figure 4.4 shows the difference between FF1 and FF2 for -CG flash with three subsequent return strokes.

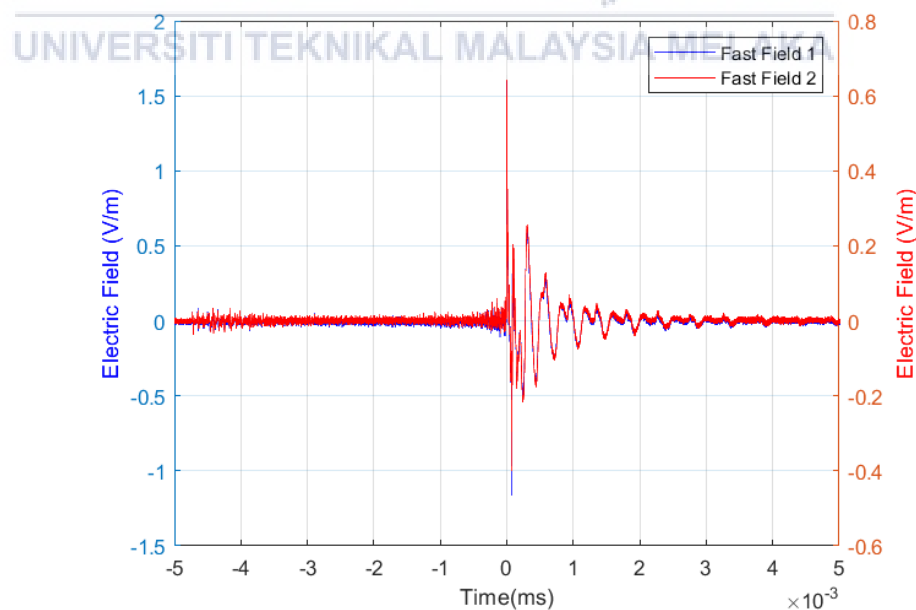


Figure 4.2: Negative cloud-to-ground flashes with single return stroke for Fast Field 1 and Fast Field 2

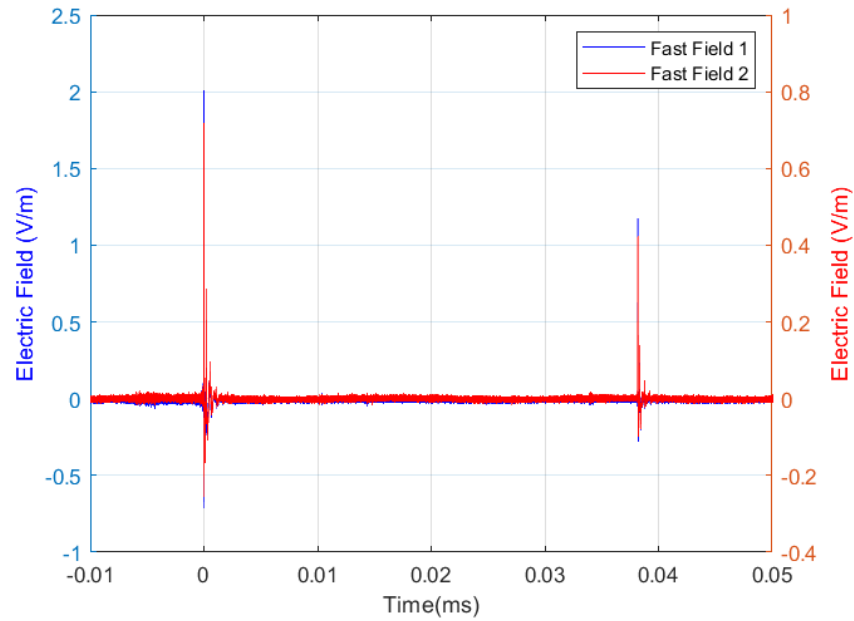


Figure 4.3: Negative cloud-to-ground flashes with two return strokes for Fast Field 1 and Fast Field 2

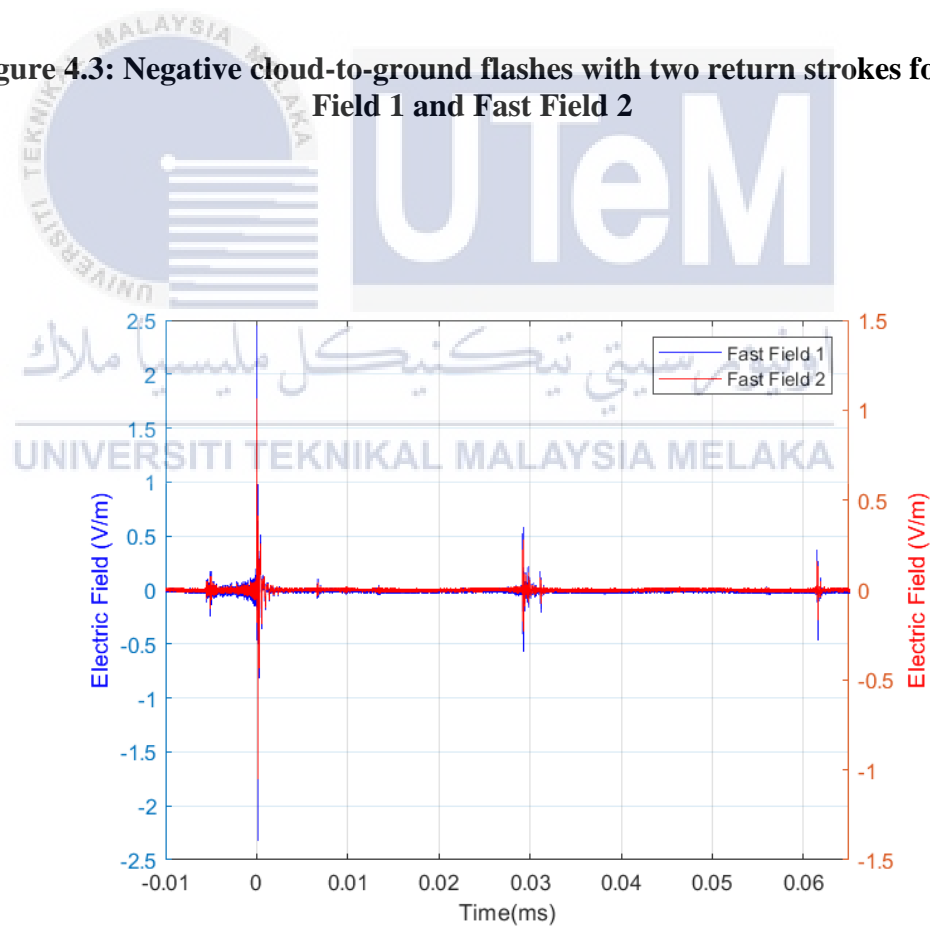


Figure 4.4: Negative cloud-to-ground flashes with three return strokes for Fast Field 1 and Fast Field 2

4.2.3 Performance similarity between Fast Field 1 and Fast Field 2

The similarity of lightning flashes between FF1 and FF2 has been shown in Figure 4.5 which both of FF1 and FF2 have their own performance which is OPA633 is a high-speed, current-feedback op-amp that's often used in applications requiring wide bandwidth and high slew rates while the BUF634 is a high-current buffer amplifier designed to provide high output current with low distortion. Due to that, the similarity in terms of performance may have quite a difference. Similar measures are used to quantify how related or close data samples are to each other. The similarity measure is usually expressed as a numerical value, typically between 0 and 1, where 0 represents low similarity (dissimilar data objects) and 1 represents high similarity (very similar data objects). The analysis of 60 samples results in a mean similarity value of 0.8266. This indicates similarity performance achieved in the 60 samples was around 83%. Through the analysis obtained, 0.9936 maximum similarity was achieved while minimum similarity is 0.7149. The parameter of similarity between FF1 and FF2 was shown in Table 4.1.

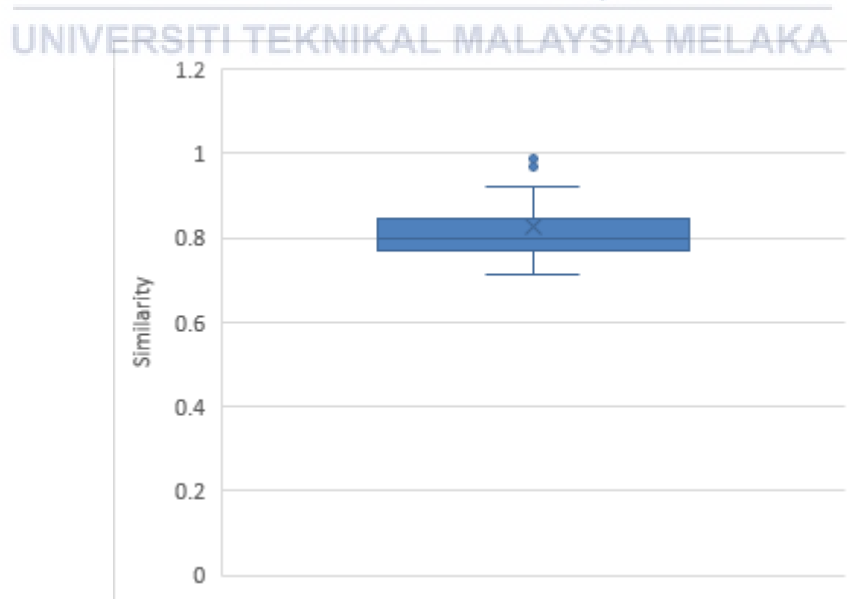


Figure 4.5: The similarity of lightning flashes between Fast Field 1 and Fast Field 2

Table 4.1: Parameter of similarity between Fast Field 1 and Fast Field 2

	Minimum	Maximum	Mean	Median	First Quartile	Third Quartile
Similarity	0.7149	0.9936	0.8266	0.7971	0.7692	0.8461

4.2.4 The characteristic performance of return stroke between Fast Field 1 and Fast Field 2

The parameter of single return stroke and multiple return stroke was analyzed based on the peak amplitude, pulse duration, zero crossing time, zero-to-peak rise time, slow front, and fast transition. The illustration of all parameters was included in Figure 4.6 until Figure 4.9. The blue box referred to FF1 which is from existing system operated by using OPA633 buffer with combination of parallel plate antenna while orange box referred to FF2 which is from current system operated by using BUF634 buffer with combination of parallel plate antenna.

Generally, these two systems have the same functionality which is detecting the lightning flash during thunderstorm event but difference in characteristic return stroke performance. Figure 4.6 and Figure 4.7 showed the comparison of the performance delivered by these two systems for single return stroke. Figure 4.6 shows the difference of peak amplitude in single return stroke where these two systems have quite a difference in electric field intensity. The mean peak amplitude of the electric field for FF1 was 2.11V, while for FF2 it was 1.0V. These values indicate that the electric field derived from BUF634 is lower than OPA633. The comparison of these values showed that the characteristic of peak amplitude is different due to specification of buffer amplifier which is BUF634 is a high-current buffer amplifier designed to provide high output current with low distortion.

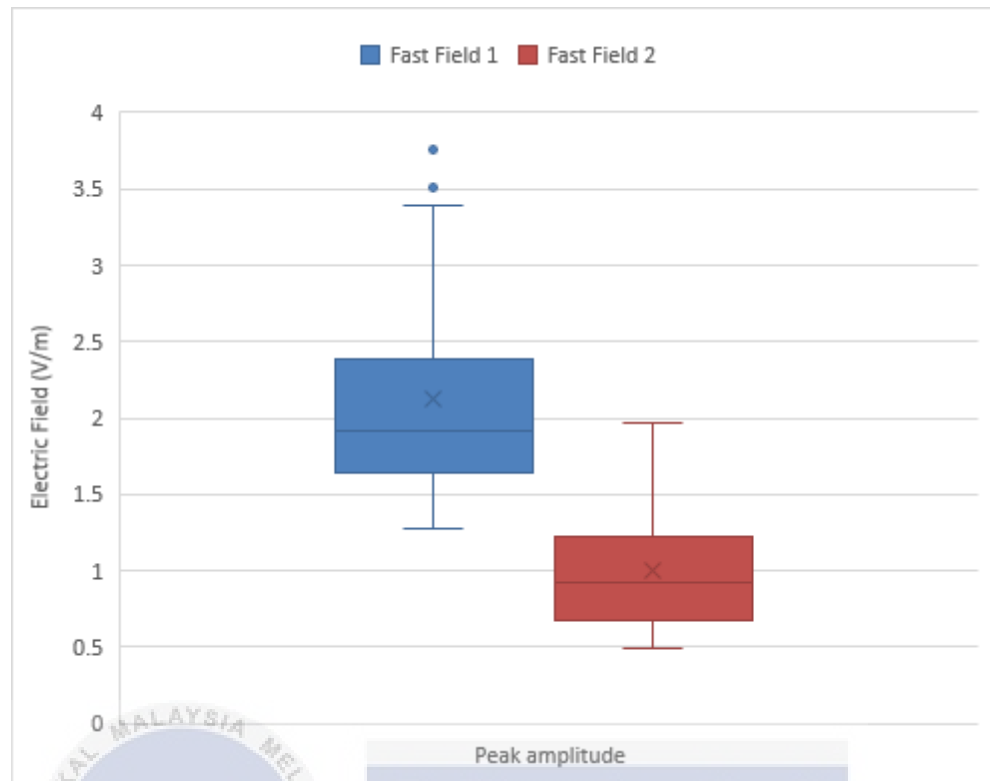


Figure 4.6: Peak amplitude of single return stroke for Fast Field 1 and Fast Field 2

Figure 4.7 shows that there are differences in the time intervals of single return stroke parameters between FF1 and FF2. Zero-to-peak rise time, slow front, and fast transition delivered almost the same performance, while pulse duration and zero crossing time delivered quite different performance. The mean pulse duration for FF1 was 97.54 μ s, while for FF2, it was 64.51 μ s. For mean zero crossing time, FF1 consists of 39.90 μ s, while FF2 consists of 23.79 μ s. The total duration of a return stroke current pulse is defined as the time interval between the return stroke start-time and return stroke end-time. Zero-to-peak rise time is the time required for a signal to cross from a specified low value to a specified high value. The mean value for FF1 was 8.04 μ s, while for FF2, it was 7.19 μ s. Slow front refers to the time it takes for a signal to rise from 10% to 90% of its final value. The mean value for FF1 was 3.94 μ s, while FF2, it

was 3.47 μ s. Fast transition refers to the time it takes for a signal to go from 20% to 80% of its final value. The mean value for FF1 was 4.1 μ s, while for FF2, it was 3.71 μ s.

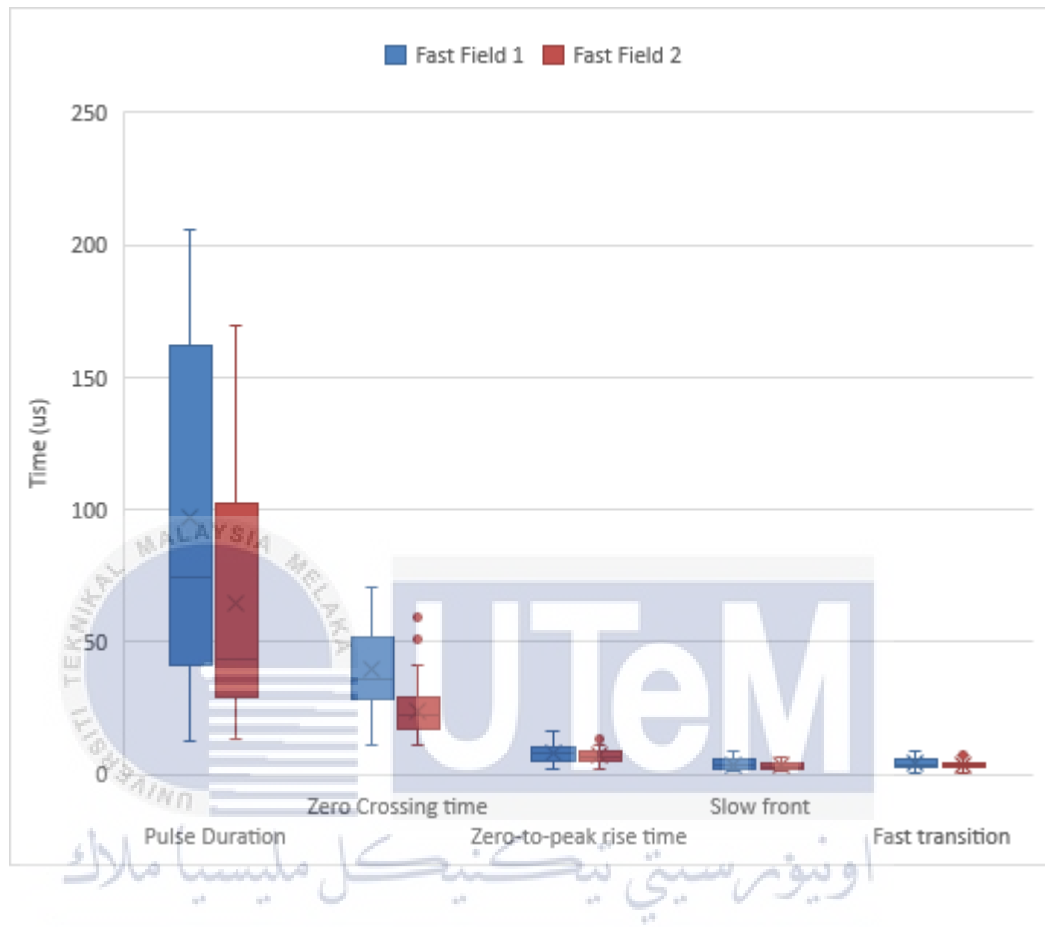


Figure 4.7: Time interval of single return stroke for Fast Field 1 and Fast Field 2

Figure 4.8 and Figure 4.9 showed the comparison of the performance delivered by these two systems for multiple return strokes. Figure 4.8 shows the difference of peak amplitude in multiple return stroke where these two systems have the same performance as single return stroke. The mean value for peak amplitude of the electric. The mean peak amplitude of the electric field for FF1 was 2.26V, while for FF2 it was 1.01V. These values indicate that the electric field on multiple return stroke is delivered with the same performance on single return stroke.

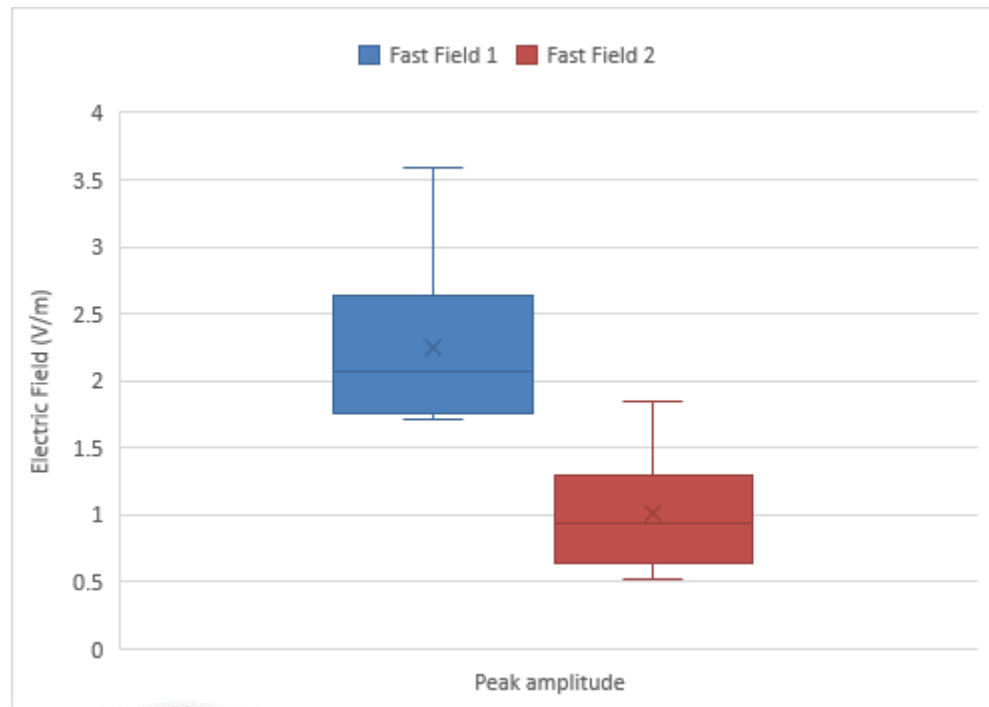


Figure 4.8: Peak amplitude of multiple return stroke for Fast Field 1 and Fast Field 2

Figure 4.9 shows that there are differences in the time intervals of single return stroke parameters between FF1 and FF2. Zero-to-peak rise time, slow front, and fast transition delivered almost the same performance, while pulse duration and zero crossing time delivered quite different performance. The mean pulse duration for FF1 was 86.47 μ s, while for FF2, it is 55.04 μ s. For mean zero crossing time, FF1 consists of 37.32 μ s, while FF2 consists of 30.39 μ s. The mean value zero-to-peak rise time for FF1 was 7.58 μ s, while for FF2, it is 8.74 μ s. The mean slow front value for FF1 was 4.75 μ s, while for FF2, it is 4.98 μ s. The mean fast transition for FF1 was 2.84 μ s, while for FF2, it is 3.77 μ s. Lastly, inter-stroke is the time interval that measures from first return stroke to the next return stroke for the lightning flashes that contain a multiple return stroke. The mean value of inter-stroke for FF1 was 48.89ms while for FF2 was 50.56ms.

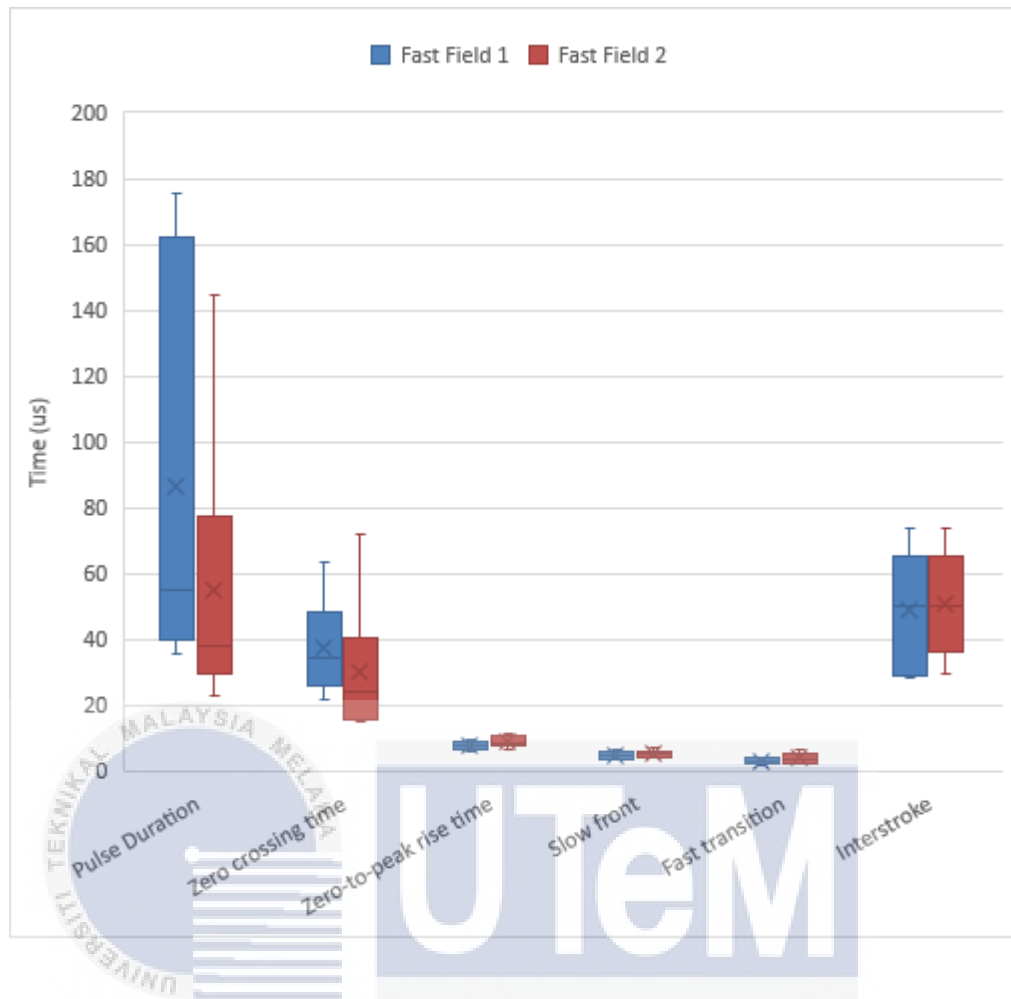


Figure 4.9: Time interval of multiple return stroke for Fast Field 1 and Fast Field 2

The provided data from Tables 4.2 to 4.7 offers a comprehensive analysis of the characteristics of both FF1 and FF2 during the first return stroke and subsequent return stroke of -CG flashes. The results reveal distinct differences in key parameters between the two fields. In Table 4.2, the peak amplitude of FF2 is notably lower than that of FF1, with a reduction of approximately 2.11 times during the first return stroke and 2.24 times during the subsequent return stroke. Table 4.3 presents data on pulse duration, showing that FF2 exhibits significantly shorter durations compared to FF1, with reductions of approximately 1.51 times during the first return stroke and 1.57 times during the subsequent return stroke. Table 4.4 reveals that the zero-crossing time

for FF2 was approximately 1.68 times shorter than that of FF1 during the first return stroke and 1.24 times shorter during the subsequent return stroke.

Additionally, Table 4.5 indicates that the zero-to-peak rise time of FF2 was approximately 1.12 times shorter during the first return stroke and 1.24 times shorter during the subsequent return stroke, as compared to FF1. Table 4.6 shows that the slow front in FF2 was 1.14 times shorter than in FF1 during the first return stroke and 1.04 times longer during the subsequent return stroke. Table 4.7 illustrates that FF2 has fast transitions that are 1.44 times shorter than FF1 during the first return stroke and 1.33 times longer during the subsequent return stroke. Lastly, Table 4.8 shows the inter-stroke in FF2 was 1.02 times shorter than FF1.

These findings collectively highlight the consistent differences in characteristics between the two fields, with FF2 generally exhibiting lower amplitudes, shorter durations, and quicker time parameters compared to FF1 during both the first and subsequent return strokes, except for the slow front in the subsequent return stroke. This data is crucial for understanding the distinct behavior of these two fields in -CG flashes, offering valuable insights into lightning flashes.

Table 4.2: Peak amplitude

	Fast Field 1		Fast Field 2	
	Single Stroke	Subsequence Stroke	Single Stroke	Subsequence Stroke
Min	1.28V	1.72V	0.49V	0.52V
Max	3.76V	3.60V	1.97V	1.85V
Mean	2.11V	2.26V	1.00V	1.01V
Median	1.92V	2.07V	0.92V	0.94V
First Quartile	1.64V	1.75V	0.68V	0.64V
Third Quartile	2.38V	2.64V	1.22V	1.29V

Table 4.3: Pulse duration

	Fast Field 1		Fast Field 2	
	Single Stroke	Subsequence Stroke	Single Stroke	Subsequence Stroke
Min	12.67us	35.51us	13.25us	23.05us
Max	205.9us	175.4us	169.7us	144.5us
Mean	97.54us	86.47us	64.51us	55.04us
Median	72.36us	54.57us	43.77us	38.03us
First Quartile	41.45us	39.96us	29.21us	29.70us
Third Quartile	162.23us	161.83us	102.43us	77.16us

Table 4.4: Zero crossing time

	Fast Field 1		Fast Field 2	
	Single Stroke	Subsequence Stroke	Single Stroke	Subsequence Stroke
Min	10.96us	21.78us	11.02us	14.74us
Max	70.80us	63.50us	59.53us	71.81us
Mean	39.90us	37.32us	23.79us	30.09us
Median	36.41us	34.07us	22.33us	24.09us
First Quartile	28.30us	26.00us	16.90us	15.65us
Third Quartile	51.50us	48.18us	29.01us	40.33us

Table 4.5: Zero-to-peak rise time

	Fast Field 1		Fast Field 2	
	Single Stroke	Subsequence Stroke	Single Stroke	Subsequence Stroke
Min	1.86us	5.89us	2.04us	6.21us
Max	16.5us	9.64us	14.99us	11.18us
Mean	8.04us	7.58us	7.19us	8.74us
Median	7.78us	7.58us	6.92us	8.41us
First Quartile	5.27us	6.32us	5.46us	7.50us
Third Quartile	10.47us	8.67us	8.55us	10.51us

Table 4.6: Slow front

	Fast Field 1		Fast Field 2	
	Single Stroke	Subsequence Stroke	Single Stroke	Subsequence Stroke
Min	1.0us	3.35us	1.15us	3.72us
Max	8.99us	6.63us	6.91us	6.73us
Mean	3.94us	4.75us	3.47us	4.98us
Median	3.74us	4.61us	3.16us	4.93us
First Quartile	1.84us	3.64us	1.76us	3.82us
Third Quartile	5.93us	5.80us	4.69us	5.91us

Table 4.7: Fast transition

	Fast Field 1		Fast Field 2	
	Single Stroke	Subsequence Stroke	Single Stroke	Subsequence Stroke
Min	0.50us	1.65us	0.85us	2.16us
Max	9.02us	4.16us	9.00us	6.68us
Mean	4.10us	2.84us	3.71us	3.77us
Median	3.37us	2.77us	3.29us	3.39us
First Quartile	2.75us	2.02us	2.49us	2.31us
Third Quartile	5.69us	3.68us	4.34us	5.15us

Table 4.8: Inter-stroke

	Fast Field 1	Fast Field 2
	Subsequence Stroke	Subsequence Stroke
Min	28.19us	29.20us
Max	73.66us	73.67us
Mean	48.89us	50.56us
Median	49.90us	49.99us
First Quartile	28.89us	35.89us
Third Quartile	65.36us	65.36us

4.2.5 Ratio of lightning flashes between Fast Field 1 and Fast Field 2

Figure 4.10 shows a ratio of lightning flashes between FF1 and FF2. A ratio is a comparison of two parameter values between FF1 and FF2. It's expressed as the quotient or fraction when one quantity is divided by another. Ratios show the relative sizes or magnitudes of two values and are often used to compare difference parameter value. The performance of the system can be evaluated by referring to the number of ratios. Based on the results obtained, peak amplitude, pulse duration, and zero crossing time have a higher ratio compared to other parameters. The mean ratio value for peak amplitude was 2.3. then pulse duration was 2.14 and zero crossing time was 1.9. These results show that the performance of peak amplitude in FF1 was 2.4 times greater than FF2, then pulse duration in FF1 was 2.14 times greater than FF2, and zero crossing time in FF1 was 1.9 times greater than FF2. The other parameters of zero-to-peak rise time, slow front, and fast transition have a mean value of 1.1, 1.16 and 1.12 respectively. The results show that the performance of parameters of zero-to-peak rise time, slow front, and fast transition have a similarity of performance between FF1 and FF2 because the number of ratios is near to 1. Table 4.9 shows the ratio value of each parameter return stroke.

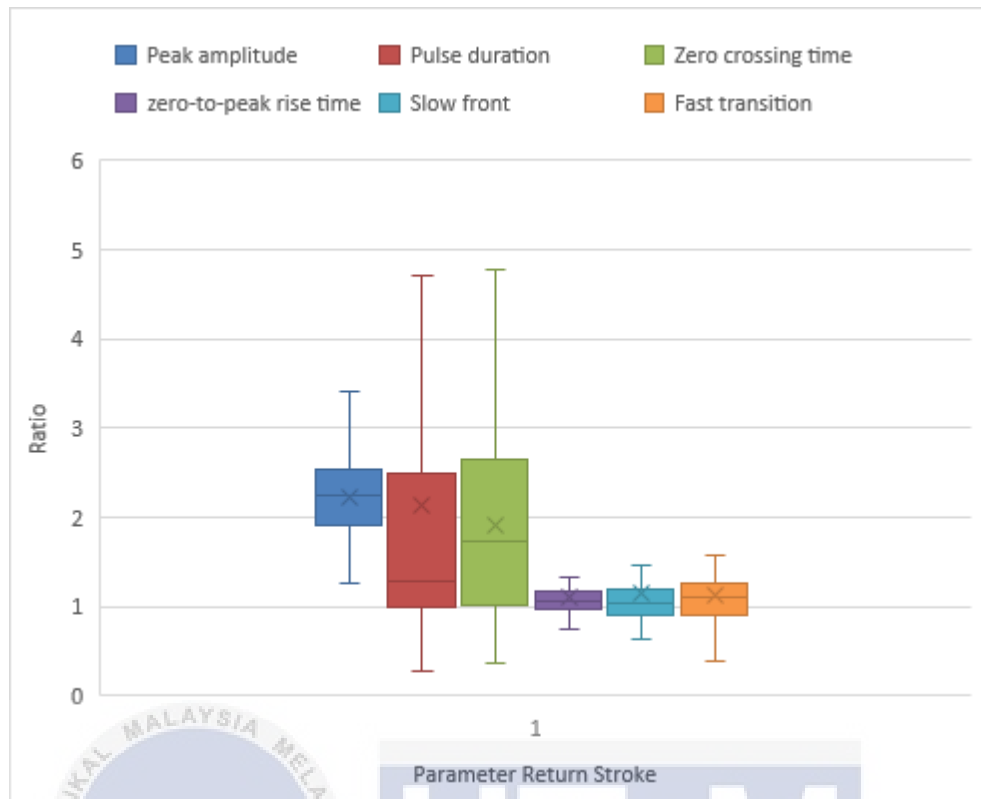


Figure 4.10: Ratio of lightning flashes between Fast Field 1 and Fast Field 2

Table 4.9: Value of ratio for each parameter return stroke

	Peak Amplitude	Pulse Duration	Zero Crossing Time	Zero-to-Peak Rise Time	Slow Front	Fast Transition
Min	1.25	0.28	0.36	0.48	0.40	0.32
Max	3.40	11.00	4.78	1.93	2.90	2.89
Mean	2.23	2.14	1.91	1.1	1.16	1.12
Median	2.24	1.29	1.74	1.05	1.04	1.09
First Quartile	1.92	0.99	1.00	0.97	0.90	0.90
Third Quartile	2.53	2.49	2.66	1.18	1.19	1.27

4.3 DISCUSSION

The lightning detection system using BUF634 in combination with a parallel plate antenna was proven, as shown in Figure 4.1, to be capable of detecting -CG flashes for single, two subsequent, and three subsequent return strokes, as well as intracloud flashes. Out of a total of 111 lightning flashes detected, 60 were identified as -CG flashes, while 51 were classified as IC. The focus of the results was on the -CG flashes, analyzing their characteristics, including peak amplitude, pulse duration, zero crossing time, zero-to-peak rise time, slow front, and fast transition. In this study, the validation of the current system using BUF634 was verified by comparing the results obtained with the existing system using OPA633.

The results obtained demonstrate significant similarities in the shape, characteristics, and overall processes between single strokes and subsequent return strokes. However, notable differences exist in key parameters. The mean peak amplitude for single strokes exhibits a 52.6% error, while subsequent return strokes show a 55.3% error. Similarly, the mean pulse duration displays a 33.86% error for single strokes and a 36.3% error for subsequent return strokes. Furthermore, the mean zero-crossing time shows a 40.3% error for single strokes and a 19.4% error for subsequent return strokes. The mean zero-to-peak rise time exhibits a 10.6% error for single strokes and a 15.3% error for subsequent return strokes. Additionally, the mean slow front demonstrates an 11.92% error for single strokes and a 4.8% error for subsequent return strokes. Lastly, the mean fast transition shows a 9.5% error for single strokes and a 32.7% error for subsequent return strokes. These performance differences are attributed to the specifications of the components, where OPA633 is a monolithic unity-gain buffer amplifier with a very wide bandwidth (260MHz) and high slew rate (2500V/us), in contrast to BUF634, which is a device operating on a

1.5-mA quiescent current with a 250-mA output, 3750-V/ μ s slew rate, and 35 MHz to 210 MHz adjusted bandwidth.

The most lightning location systems impose a limitation on the maximum number of discharges, typically set at 15. There were found 94 trains of radio signals of lightning flashes from 4 thunderstorms in 2010-2012 years of observation over Yakutia. Lightning was found to be able to contain about 11 return strokes. Moreover, the percentage of flashes containing more than 15 strokes ranges from 2.6% to 4.8%. Notably, the maximum multiplicity tends to slightly increase with a decrease in latitude. In general, the first stroke within a lightning flash is the most significant due to the substantial amount of charge required to initiate a discharge between the Earth and the cloud. The amplitude exhibits an increasing trend from the first stroke to subsequent strokes, followed by a reduction in amplitude towards the last stroke. It was noted that although the first stroke typically holds the highest amplitude, a second stroke with a maximum amplitude (though not exceeding that of the first) may occur, followed by a gradual decrease in amplitude until the final stroke.

The research emphasized that since all signals from a single lightning event originate from the same distance within a short time frame, variations in propagation conditions can be neglected. Consequently, the atmospheric magnitude transformation from stroke to stroke was considered negligible in the analysis [34]. In Malaysia during the flash flood thunderstorm recorded a maximum multiplicity of 14 return strokes was observed in Malaka. There were 337 CG flashes detected and the maximum number of return strokes detected by the Field Antenna (FA) system was 14 [35]. For analysis on the number of return strokes, the system detected a total of 60 -CG flashes, with the highest number of return strokes recorded being 3. However, the

prevalent pattern among CG flashes consisted of 1 return stroke which was 54. Only a minority of samples had two and three return strokes which were four and two of flashes respectively. Furthermore, Figure 4.6 illustrates the diminishing trend in the maximum peak amplitude from the first return stroke to the third return stroke.

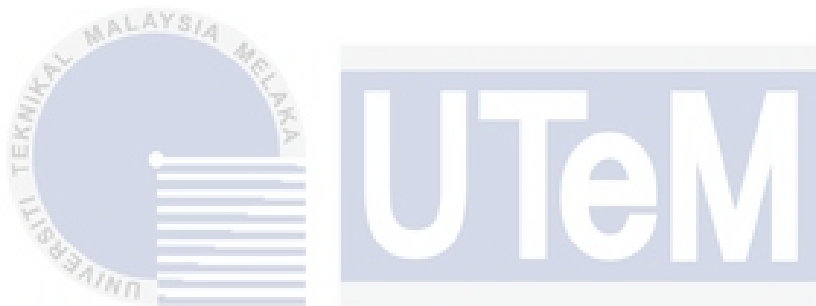
The initial occurrence of a lightning flash with two subsequent return strokes took place on July 11, 2024, at 01:44:00. In this instance, the inter-stroke duration between the first and second return strokes was measured at 28.19ms. Another lightning flash with two subsequent return strokes was observed later that day at 07:11:00, exhibiting an inter-stroke duration between the first and second return strokes was 62.59ms. A subsequent lightning flash with two subsequent return strokes occurred at 07:28:00 on the same day, and it featured an inter-stroke duration between the first and second return strokes was 59.68ms. Additionally, another lightning flash with two subsequent return strokes was documented at 07:33:00 on the same day, with an inter-stroke duration between the first and second return strokes measured at 40.12ms. Besides that, three subsequent return strokes occurred at same day at 01:41:00 and 02:02:00 where at 01:41:00 the value of inter-stroke between first and second return strokes is 73.66ms while between second and third return stroke was 2.36ms. then, at 02:02:00 the value of inter-stroke between first and second return stroke is 29.12ms while between second and third return strokes was 32.14ms.

4.4 SUMMARY

This chapter delves into an extensive analysis of negative cloud-to-ground -CG lightning flashes, segmented into single, double, and triple return stroke events, comparing signals captured by FF1 and FF2 using circuit designs involving OPA633 and BUF634. Among 111 detected lightning flashes, 60 were -CG and 51 were intracloud IC flashes, with the primary focus on -CG events, evaluating critical parameters like peak amplitude, pulse duration, zero crossing time, zero-to-peak rise time, slow front, and fast transition. The comparison highlighted distinct variations in peak amplitude, pulse duration, and zero crossing time between FF1 and FF2, showing FF1 values were roughly 2.3 times, 2.14 times, and 1.9 times greater, respectively, while zero-to-peak rise time, slow front, and fast transition displayed values closer to 1, indicating a more comparable performance between FF1 and FF2 for these parameters. The analysis also utilized a similarity measure, revealing an overall 83% similarity between FF1 and FF2, with variations between 0.7149 and 0.9936 across the dataset, demonstrating differing degrees of similarity in lightning flash characteristics between the two fields.

CHAPTER 5

CONCLUSION AND FUTURE WORKS



5.1 CONCLUSION

The primary goal of the project was to design a low-cost system that can capture lightning events within the frequency range of 1Hz to 10MHz and to analyze the type of lightning flashes with their characteristic performance. The objective of the project has been achieved and fully met where the system has been designed and test the functionally to detect the lightning flashes by analyze the type of lightning with their return stroke parameter and characteristic performance. This project was compared with the existed system that using OPA633 to determine the validation and performance with the current system by using BUF634. Overall, of the comparison was shown that there are quite different in system characteristic performance but the system able to detect same shape and process of lightning flashes.

The system able to detect 60 of -CG and 51 of IC lightning flashes. -CG flashes were captured on July 11, 2023, from 01:32:00 until 08:30:00 with three different characteristics where 54 were single return stroke flashes, four were two subsequent return strokes flash, and two were three subsequent return stroke flash. According to the analysis, the comparative analysis between the BUF634 and OPA633 in lightning detection systems revealed an 83% similarity in lightning flash detection capability. While both exhibit similar characteristics in zero-to-peak rise time, slow front, fast transition, and inter stroke detection, notable differences exist. The BUF634 demonstrates a 2.3 times lower peak amplitude, a 2.1 times shorter pulse duration, and 1.9 times shorter zero crossing time compared to the OPA633. Despite these variations, the BUF634 proves capable of detecting similar types of lightning flashes -CG and IC, showcasing potential cost-effectiveness without compromising crucial detection capabilities.

5.2 FUTURE WORK

5.2.1 Internet of Things (IoT)

The future development of a low-cost lightning detection system could be significantly enhanced by leveraging IoT (Internet of Things) technologies [36]. The incorporation of IoT technologies would enable seamless remote monitoring and control of the lightning detection system, allowing for efficient and centralized management [37]. Moreover, the implementation of wireless communication protocols can further elevate the system's capabilities by facilitating swift and reliable data transmission. This not only ensures the timely dissemination of critical information but also enables real-time alerts to be delivered to relevant authorities or

stakeholders [38]. By harnessing these technological advancements, the low-cost lightning detection system can achieve heightened responsiveness, improved accessibility, and a more robust communication infrastructure, ultimately contributing to its overall effectiveness in providing accurate and timely lightning event information.

IoT technology enables real-time data collection and transmission, allowing lightning detection systems to gather and transmit data instantly. With IoT capabilities, operators can remotely monitor and manage the detection system from anywhere, enabling prompt responses to changing conditions or issues. IoT-enabled systems can also utilize cloud computing for data storage and analysis, providing valuable insights for weather monitoring and predictive analysis. Lastly, IoT can improve the accuracy of lightning detection by incorporating multiple sensors and leveraging data fusion techniques. This leads to more precise identification and characterization of lightning events.



5.2.2 Artificial Intelligence (AI)

The future development of a low-cost lightning detection system involves the implementation of an artificial intelligence [39]. By integrating machine learning algorithms into the system, real-time lightning event classification based on waveform analysis can be achieved, significantly enhancing the system's capability to differentiate between various types of lightning strikes [40]. Furthermore, the development of specialized algorithms aimed at distinguishing between natural and human-made electromagnetic interference holds the potential to mitigate false positives in lightning detection, thus refining the system's accuracy and reliability.

This innovative approach not only ensures a more nuanced understanding of lightning events but also contributes to the overall efficiency and effectiveness of the low-cost detection system [41].

AI algorithms can discern intricate patterns in lightning data, distinguishing between various types of lightning strikes, their frequencies, and intensities. This enables more precise and detailed analysis of lightning events. AI models can also forecast lightning strikes by analyzing historical data patterns, weather conditions, and atmospheric variables, allowing for advanced warning systems and improved preparedness for potential lightning-related hazards. Additionally, AI enables lightning detection systems to make real-time decisions, such as triggering specific actions when a storm is approaching. Over time, these systems can adapt and learn from new data, refining their detection and analysis methods to become more efficient and accurate in identifying lightning events.

REFERENCES

- [1] V. Mansoor, "Throwing light on lightning," 2021.
- [2] M. Z. A. Ab Kadir, N. R. Misbah, C. Gomes, J. Jasni, W. W. Ahmad and M. K. Hassan, "Recent statistics on lightning fatalities in Malaysia," 2012.
- [3] T. Christophides, "Cardiac Effects of Lightning Strikes," 2017.
- [4] A. K. Adzhiev, "Lightning detection system in the North Caucasus," 2013.
- [5] P. M. Bitzer, "A bayesian Approach to assess the performance of lightning detection system," 2015.
- [6] A. Y. Kostinskiy, "Observations of the connection of positive and negative leaders in meter-scale electric discharges generated by clouds of negatively charged water droplets," 2016.
- [7] D. Rodriguez-Sanabria, "Lightning and Lightning Arrester Simulation in Electrical Power Distribution Systems," 2005.
- [8] A. Kalair, "Lightning Interactions with Humans and Lifelines," 2013.
- [9] S. Shivalli, "Lightning Phenomenon, Effects and Protection of Structures," 2016.

- [10] V. A. Rakov, "Positive and bipolar lightning discharges to ground," pp. 214-550, 2003.
- [11] S. Singer, *The nature of ball lightning*, Springer Science & Business Media., 2012.
- [12] T. Shindo, "Lightning striking characteristics to tall structures," *IEEJ Transactions on Electrical and Electronic Engineering*, pp. 938-947, 2018.
- [13] J. R. Dwyer and M. A. Uman, "The physics of lightning," *Physics Reports*, 2014.
- [14] S. Shivalli, "Lightning Phenomenon, Effects and Protection of Structures from lightning," *Journal of Electrical and Electronics Engineering*, vol. 11, no. 3Ver. I (May. – Jun. 2016), pp. 44-50, 2016.
- [15] A. Nag and V. A. Rakov, "Positive lightning: An overview, new observations, and inferences," *Journal of Geophysical Research*, vol. 117, 2012.
- [16] S. Marcelo, C. Leandro and K. Philip, "High-speed video observations of positive ground flashes produced by intracloud lightning," *Geophysical research letters*, 2009.
- [17] M. Thomas, S. Maribeth, K. Sumedhe, C. Steve, L. Gaopeng, B. Hans-Dieter, B. Michael, C. Valerie and X. Shaolin, "Initial breakdown pulses in intracloud lightning flashes and their relation to terrestrial gamma ray flashes," *GEOPHYSICAL RESEARCH*, vol. 118, 2013.
- [18] M. Akinyemi, M. Emetere, A. Boyo and M. Usikalu, "Lightning a fundamental of atmospheric electricity," 2014.

- [19] A. M. Yusof, "Lightning generated electric field over land and sea at Northern," pp. 457-464, 2020.
- [20] A. H. Faranadia, "Measurement of Negative Lightning Return Strokes Using a Proposed Small-Scale Parallel Plate Antenna at the Central," 2021.
- [21] N. A. Ramlee, "Investigation on Antenna Material and Operational Amplifier Model for Measuring Electric Fields from Lightning Flashes," 2022.
- [22] P. B. Adhikari, "Feature of positive ground flashes observed in Kathmandu Nepal," 2015.
- [23] D. U. J. Sonnadara, C. M. Edirisinghe and I. M. K. Fernando, "Construction of a High Speed Buffer Amplifier to Measure Lightning Generated Vertical Electric Fields," pp. 21-29, 2001.
- [24] S. A. S. Baharin, "Electric Field Waveforms of Very Close Negative," 2020.
- [25] H. E. Rojas, "New Circuit for the Measurement of Lightning Generated Electric Fields," 2017.
- [26] L. Aguirre, "A low-cost lightning electric field measurement device for tropical zone: An initial result.," 2022.
- [27] W. I. Ibrahim, "Measurement of Vertical Electric Fields from lightning Flashes using Parallel Plate Antenna," 2015.
- [28] E. H. Lay, "Investigating Lightning-to-Ionosphere Energy Coupling Based on VLF Lightning Propagation Characterization," 2008.

- [29] Z. Yanan, R. A. Vladimir and T. D. Manh, "Unusual electric field waveforms produced by negative lightning strokes terminated on a 257-m tower," 2016.
- [30] V. Cooray, "An introduction to lightning," vol. 201, 2015.
- [31] S. A. Mohammad, M. R. Ahmad, M. Abdullah, P. Sangjong, S. A. Shamsul Baharin, N. Yusop, G. Lu and V. Cooray , "Characteristics of Lightning Electromagnetic Fields Produced by Antarctica Storms," April 2022.
- [32] N. Yusop, "Cloud-to-Ground lightning observations over the Western Antarctic region," 2019.
- [33] N. Abdullah, M. P. Yahaya and N. S. Hudi, "Implementation and use of lightning detection network in Malaysia," IEEE 2nd International Power and Energy Conference, 2008.
- [34] Tarabukina, "Statistics on characteristics of lightning with several return strokes in Yakutia," 2014.
- [35] N. Yusop, "Correlation analysis between lightning flashes and rainfall rate during a flash flood thunderstorm," 2022.
- [36] S. R. Govinda K, "Review on IOT technologies," *International Journal of Applied Engineering Research*, pp. 2848-2856, 2016.
- [37] A. Gharaibeh, M. A. Salahuddin, S. J. Hussini, A. Khreishah, I. Khalil, M. Guizani and A. Al-Fuqaha, "Smart cities: A survey on data management, security, and enabling technologies," *IEEE Communications Surveys & Tutorials*, pp. 2456-2501, 2017.

- [38] A. Salh, L. Audah, N. S. M. Shah, A. Alhammadi, Q. Abdullah, Y. H. Kim and A. A. Almohammed, "A survey on deep learning for ultra-reliable and low-latency communications challenges on 6G wireless systems," *IEEE Access* 9, pp. 55098-55131, 2021.
- [39] E. S. Brunette, R. C. Flemmer and C. L. Flemmer, "A review of artificial intelligence," pp. 385-392, 2009.
- [40] X. Zhang, C. Wang and Y. Tian, "Classification and Feature Extraction of Lightning Electric Field Waveforms Based on Machine Learning," *IEEE 2nd International Conference on Computer Communication and Artificial Intelligence (CCAI)*, pp. 199-204, 2022.
- [41] I. Ullah, M. N. R. Baharom, H. Ahmad, F. Wahid, H. M. Luqman, Z. Zainal and B. Das, "Smart lightning detection system for smart-city infrastructure using artificial neural network. *Wireless Personal Communications*," *Wireless Personal Communications*, pp. 1743-1766., 2019.
- [42] C. V, "Mechanism of the lightning flash," The institution of Engineering and Technology, London, United Kingdom, 2014.

APPENDICES

Appendix A: Data analysis of negative cloud-to-ground parameter in Fast Field 1

Name	Peak Amplitude (V)	Pulse Duration (uS)	Zero Crossing time (uS)	Zero-to-Peak Rise Time (uS)	Slow Front (uS)	Fast Transition (uS)	Return Stroke	Interstroke	
								1st and 2nd (mS)	2nd and 3rd (mS)
July_(181)	1.098	163.3	41.43	14.99	5.985	9.005	1	0	0
July_(183)	0.62	34.74	28.74	5.149	1.447	3.702	1	0	0
July_(205)	0.582	38.62	29.62	5.21	2.306	2.904	1	0	0
July_(209)	0.625	100.7	24.81	4.379	1.338	3.041	1	0	0
July_(218)	0.582	56.32	31.95	5.757	2.662	3.095	1	0	0
July_(245)	0.92	43.44	21.72	10.54	6.388	4.152	1	0	0
July_(269)	0.617	93.47	39.44	6.21	2.833	3.377	1	0	0
July_(336)	1.258	169.7	20.57	7.318	5.143	2.175	1	0	0
July_(337)	0.633	28.46	17.06	7.838	3.61	4.228	1	0	0
July_(357)	1.815	69.17	23.63	6.825	4.559	2.226	1	0	0
July_(359)	0.726	24.54	15.21	5.889	3.067	2.722	1	0	0
July_(365)	0.915	16.82	13.59	5.014	2.851	2.163	1	0	0
July_(388)	0.6	22.28	15.99	10.17	4.641	5.529	1	0	0
July_(409)	0.61	75.71	24.94	10.43	6.239	4.191	1	0	0
July_(416)	0.861	26.54	11.51	3.887	1.451	2.436	1	0	0
July_(418)	0.821	16.41	12.84	4.31	1.593	2.717	1	0	0

July_(419)	0.762	29.24	16.98	7.436	4.924	2.512	1	0	0
July_(426)	0.662	41.74	20.42	7.941	4.095	3.846	1	0	0
July_(431)	0.526	29.13	19.34	10.74	4.609	6.131	1	0	0
July_(437)	0.752	19.39	15.69	6.754	3.05	3.704	1	0	0
July_(438)	0.908	51.56	15.08	6.944	3.904	3.04	1	0	0
July_(446)	0.988	138.4	31.89	13.21	6.91	6.3	1	0	0
July_(450)	0.693	44.1	29.88	6.9	1.154	5.746	1	0	0
July_(451)	1.358	33.65	14.56	9.501	6.6	2.901	1	0	0
July_(462)	1.662	23.16	20.99	8.586	5.824	2.899	1	0	0
July_(479)	1.172	129	29.94	6.563	2.625	3.938	1	0	0
July_(488)	0.832	107.6	19.55	6	4.162	1.838	1	0	0
July_(507)	0.681	114.2	16.32	5.874	2.962	2.912	1	0	0
July_(513)	0.833	97.29	28.98	3.457	1.215	2.242	1	0	0
July_(531)	0.982	31.16	18.65	4.835	1.201	3.634	1	0	0
July_(536)	0.98	42.48	29.11	11.27	5.865	5.405	1	0	0
July_(554)	1.197	119.2	25.11	6.183	1.492	4.691	1	0	0
July_(559)	0.923	25.95	16.66	10.21	5.325	4.885	1	0	0
July_(569)	0.599	46.42	23.07	8.815	1.818	6.997	1	0	0
July_(588)	1.514	134.5	22.56	8.539	6.146	2.393	1	0	0
July_(590)	1.069	53.65	22	5.169	1.16	4.009	1	0	0
July_(592)	0.72	33.58	27.28	6.974	3.776	3.198	1	0	0
July_(602)	1.348	157.4	31.3	7.541	2.629	4.912	1	0	0
July_(609)	1.17	31.87	20.33	7.41	3.213	4.197	1	0	0
July_(630)	1.152	39.96	19.99	3.691	1.79	1.901	1	0	0
July_(635)	1.966	35.12	18.73	7.021	4.083	2.938	1	0	0
July_(654)	1.794	19.55	16.52	5.808	3.687	2.121	1	0	0
July_(660)	1.609	15.16	11.02	3.968	2.606	1.362	1	0	0
July_(661)	1.314	66.56	23.72	8.101	6.678	1.423	1	0	0
July_(662)	1.208	39.41	22.1	5.54	3.313	2.227	1	0	0
July_(667)	0.89	40.2	23.46	7.116	4.586	2.53	1	0	0
July_(669)	1.129	50.8	22.64	4.528	1.289	3.239	1	0	0
July_(670)	1.489	124.7	31.81	7.444	4.112	3.332	1	0	0
July_(673)	1.415	131.4	28.74	13.2	4.846	8.354	1	0	0
July_(158)	0.49	146.7	59.53	7.191	1.657	5.534	1	0	0
July_(159)	0.956	72.08	51.04	10.27	3.115	7.155	1	0	0
July_(192)	0.645	129.5	31.18	5.6	1.616	3.984	1	0	0

July_(212)	1.66	13.25	11.18	2.037	1.185	0.852	1	0	0
July_(594)	0.882	44.4	24.15	5.707	2.216	3.491	1	0	0
July_(162)	0.679	54.71	29.84	10.28	5.64	4.64	2	38.12	0
July_(620)	1.106	43.39	24.73	7.935	5.365	2.57	2	62.59	0
July_(156)	0.521	144.5	71.81	11.18	4.5	6.68	3	73.67	2.354
July_(190)	0.99	32.67	23.45	7.926	3.72	4.206	3	29.2	32.32
July_(652)	0.895	23.05	15.95	8.881	6.726	2.155	2	40.12	0
July_(643)	1.847	31.92	14.74	6.213	3.853	2.36	2	59.68	0



اونيورسيتي تيكنيكل مليسيا ملاك

UNIVERSITI TEKNIKAL MALAYSIA MELAKA

Appendix B: Data analysis of negative cloud-to-ground parameter in Fast Field 2

Name	Peak Amplitude (V)	Pulse Duration (uS)	Zero Crossing time (uS)	Zero-to-Peak Rise Time (uS)	Slow Front (uS)	Fast Transition (uS)	Return Stroke	Interstroke	
								1st and 2nd (mS)	2nd and 3rd (mS)
July_(181)	2.646	161.8	39.63	13.7	7.152	6.548	1	0	0
July_(183)	1.7	36.09	25.12	4.365	1.218	3.147	1	0	0
July_(205)	1.434	39.48	28.49	4.887	1.673	3.214	1	0	0
July_(209)	1.504	101.05	25.13	4.523	1.44	3.083	1	0	0
July_(218)	1.28	54.77	27.16	4.833	2.092	2.741	1	0	0
July_(245)	2.226	44.14	21.62	9.957	6.818	3.139	1	0	0
July_(269)	1.632	26.02	22.9	6.338	3.444	2.894	1	0	0
July_(336)	3.193	180	46.2	7.64	4.885	2.755	1	0	0
July_(337)	1.797	159.6	70.8	9.778	3.124	6.654	1	0	0
July_(357)	3.344	178.9	32.03	8.402	2.902	5.5	1	0	0
July_(359)	2.208	56.39	43.03	11.32	8.876	2.444	1	0	0
July_(365)	2.191	56.25	53.48	5.823	2.847	2.976	1	0	0
July_(388)	1.581	35.48	31.81	11.25	5.568	5.682	1	0	0
July_(409)	1.772	76.19	45.76	11.41	7.362	4.048	1	0	0
July_(416)	2.263	132.7	46.38	5.93	2.465	3.465	1	0	0
July_(418)	2.077	115.8	48.94	5.178	1.726	3.452	1	0	0
July_(419)	1.841	42.93	39.19	8.113	5.117	2.996	1	0	0
July_(426)	1.769	68.04	65.24	10.46	4.518	5.942	1	0	0
July_(431)	1.55	117.4	66.5	11.85	5.912	5.938	1	0	0
July_(437)	1.773	127.5	35.28	7.92	3.249	4.671	1	0	0
July_(438)	2.318	51.94	36.48	11.51	3.138	8.372	1	0	0
July_(446)	2.918	175.3	59.69	16.5	7.481	9.019	1	0	0
July_(450)	1.64	42.54	34.68	8.803	2.846	5.957	1	0	0
July_(451)	3.353	33.41	28.83	9.669	6.289	3.38	1	0	0
July_(462)	3.532	39.93	35.9	8.719	5.969	2.75	1	0	0
July_(479)	2.706	168.7	53.04	8.229	3.12	5.109	1	0	0
July_(488)	1.801	154.1	52.5	6.265	3.927	2.338	1	0	0
July_(507)	1.641	122.3	64.53	10.49	6.4	4.09	1	0	0
July_(513)	1.617	122.8	51.17	3.665	1.38	2.285	1	0	0

July_(531)	2.01	28.92	24.17	5.191	2.881	2.31	1	0	0
July_(536)	2.239	72.93	65.23	12.44	6.505	5.935	1	0	0
July_(554)	2.164	174.8	35.94	6.702	1.523	5.179	1	0	0
July_(559)	1.935	64.64	45.62	10.86	5.131	5.729	1	0	0
July_(569)	1.386	116.6	63.46	8.934	1.318	7.616	1	0	0
July_(588)	2.377	83.27	35.12	15.9	8.989	6.911	1	0	0
July_(590)	1.858	48.47	36.33	5.907	0.997	4.91	1	0	0
July_(592)	1.364	180.2	42.49	7.175	3.812	3.363	1	0	0
July_(602)	2.473	205.9	45.35	13.06	6.675	6.385	1	0	0
July_(609)	2.358	180.6	55.67	8.758	3.884	4.874	1	0	0
July_(630)	2.097	38.63	30.33	3.828	1.873	1.955	1	0	0
July_(635)	3.762	34.73	19.26	5.299	1.618	3.681	1	0	0
July_(654)	3.514	41.29	31.98	6.392	4.45	1.942	1	0	0
July_(660)	2.131	166.8	52.63	7.649	6.093	1.556	1	0	0
July_(661)	2.559	163.7	44.63	8.329	6.954	1.375	1	0	0
July_(662)	2.402	38.71	31.06	5.86	2.73	3.13	1	0	0
July_(667)	1.551	189	64.06	6.878	4.828	2.05	1	0	0
July_(669)	1.586	55.63	23.07	4.493	1.447	3.046	1	0	0
July_(670)	1.896	190	31.81	8.285	4.553	3.732	1	0	0
July_(673)	1.769	176	27.73	13.7	5.286	8.414	1	0	0
July_(158)	1.668	41.5	21.23	3.838	1.323	2.515	1	0	0
July_(159)	1.75	71.78	25.9	4.977	2.277	2.7	1	0	0
July_(192)	1.378	128.7	20.63	4.26	1.458	2.802	1	0	0
July_(212)	3.394	12.67	10.96	1.857	1.359	0.498	1	0	0
July_(594)	1.535	40.12	38.25	6.097	2.001	4.096	1	0	0
July_(162)	1.874	53.79	27.41	9.644	5.481	4.163	2	28.19	0
July_(620)	2.325	175.4	63.5	8.345	5.526	2.819	2	62.594	0
July_(156)	1.716	55.35	29.14	5.886	3.744	2.142	3	73.66	2.36
July_(190)	2.265	35.51	21.78	6.868	3.346	3.522	3	29.12	32.14
July_(652)	1.762	41.44	39	8.288	6.634	1.654	2	40.12	0
July_(643)	3.594	157.3	43.07	6.465	3.741	2.724	2	59.68	0

Appendix C: MATLAB code for cross correlation

```
start_index = 1900000;  
end_index = 2100000;  
a = A(start_index:end_index);  
b = B(start_index:end_index);  
[r,l] = xcorr(a,b,'normalized');  
Similarity=max(r);
```

